We are IntechOpen,
the world's leading publisher of
Open Access books
Built by scientists, for scientists

6,900
Open access books available

185,000
International authors and editors

200M
Downloads

Our authors are among the

154
Countries delivered to

TOP 1%
most cited scientists

12.2%
Contributors from top 500 universities

BOOK CITATION INDEX
CLARIVATE ANALYTICS
INDEXED

WEB OF SCIENCE™

Selection of our books indexed in the Book Citation Index
in Web of Science™ Core Collection (BKCI)

Interested in publishing with us?
Contact book.department@intechopen.com

Numbers displayed above are based on latest data collected.
For more information visit www.intechopen.com

Near-Infrared Spectroscopy (NIRS): A Novel Tool for Intravascular Coronary Imaging

Marie-Jeanne Bertrand, Philippe Lavoie-L'Allier and
Jean-Claude Tardif

Additional information is available at the end of the chapter

Abstract

Acute coronary syndrome (ACS) arising from plaque rupture is the leading cause of mortality worldwide. Near-infrared spectroscopy (NIRS) combined with intravascular ultrasound (NIRS-IVUS) is a novel catheter-based intravascular imaging modality that provides a chemogram of the coronary artery wall, which enables the detection of lipid core and specific quantification of lipid accumulation measured as the lipid-core burden index (LCBI) in patients undergoing coronary angiography. Recent studies have shown that NIRS-IVUS can identify vulnerable plaques and vulnerable patients associated with increased risk of adverse cardiovascular events, whereas an increased coronary plaque LCBI may predict a higher risk of future cardiovascular events and periprocedural events. NIRS is a promising tool for the detection of vulnerable plaques in CAD patients, PCI-guidance procedures, and assessment of lipid-lowering therapies. Previous trials have evaluated the impact of statin therapy on coronary NIRS defined lipid cores, whereas NIRS could further be used as a surrogate end point of future ACS in phase II clinical trials evaluating novel anti-atheromatous drug therapies. Multiple ongoing studies address the different potential clinical applications of NIRS-IVUS imaging as a valuable tool for coronary plaque characterization and predictor of future coronary events in CAD patients.

Keywords: near-infrared spectroscopy (NIRS), intravascular ultrasound (IVUS), thin-cap fibroatheroma (TCFA), acute coronary syndrome (ACS), vulnerable plaque

1. Introduction

Coronary artery disease (CAD) is the leading cause of global mortality and the rupture of an unstable atherosclerotic plaque precedes the majority of acute coronary syndromes (ACS) [1, 2]. Autopsy studies have shown that the putative substrate for most ACS and many cases of sudden

cardiac death (SCD) is the rupture of a thin-cap fibroatheroma (TCFA), the so-called *"vulnerable plaque,"* which is defined by a large lipid-rich necrotic core (NC) infiltrated with abundant macrophages and separated from the bloodstream by a thin fibrous cap [3, 4]. The ability to accurately detect index lesions using intravascular imaging is a potential attractive strategy, although it still remains a challenge in daily practice. Conventional coronary angiography (CCA) has been and continues to be an invaluable tool for epicardial coronary stenoses assessment and treatment [5]. Since the coronary angiogram provides a limited *"luminogram"* view of the coronary arteries, it cannot assess the properties of the arterial wall and thus tends to underestimate the true magnitude of plaque burden, especially in early stages of the disease in which positive vascular remodeling leads to a normal lumen caliber appearance on angiography despite substantial vascular wall plaque [6, 7]. Moreover, angiography provides no information in regard to plaque composition and biological activity, whereas intravascular imaging can potentially circumvent those limitations [8]. Several intravascular-imaging modalities, such as angioscopy, intravascular ultrasound (IVUS), virtual histology (VH), optical coherence tomography (OCT), and near-infrared spectroscopy (NIRS), have been developed throughout the quest of vulnerable plaque to characterize plaque composition and progression, to optimize patient risk stratification and for guiding therapy [9].

Near-infrared spectroscopy (NIRS) is a novel intravascular-imaging modality that provides chemical assessment related to the presence of cholesterol esters in lipid cores and
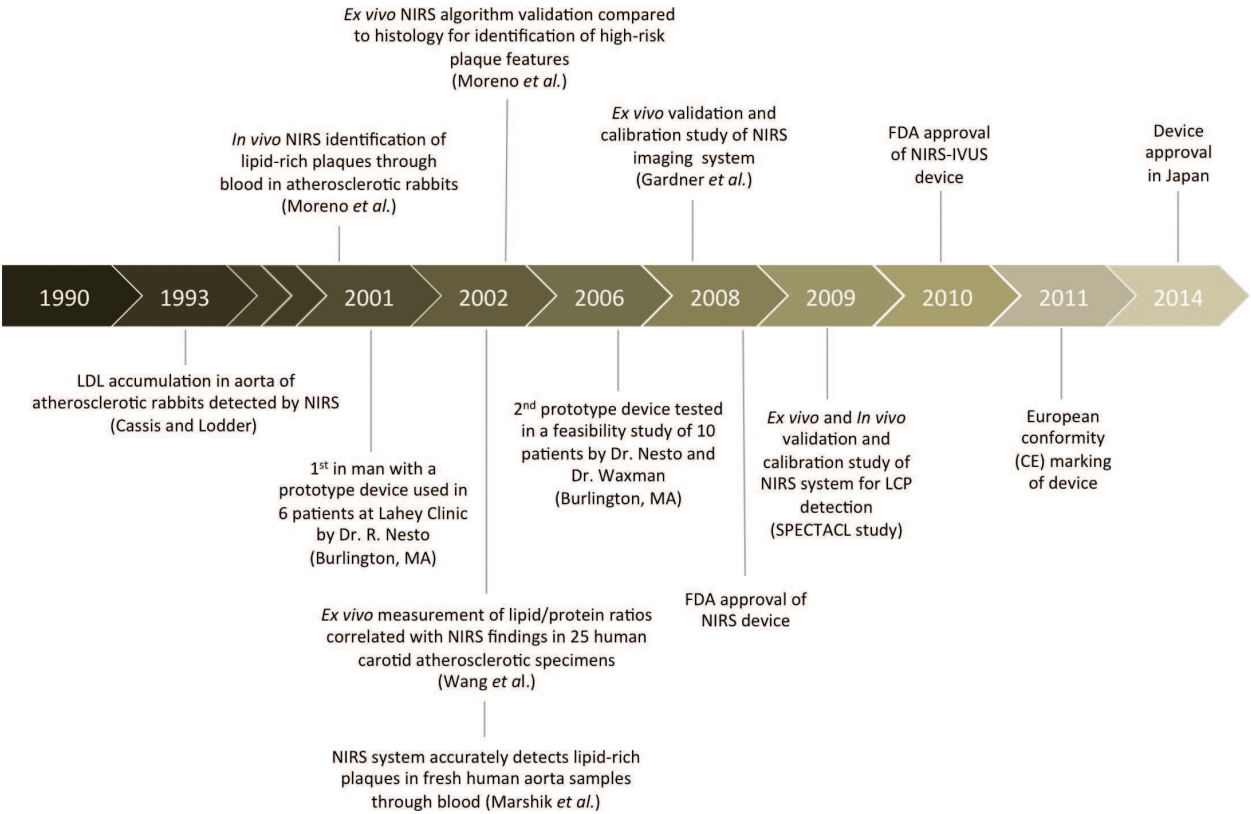

Figure 1. Timeline regarding important steps toward NIRS-IVUS imaging system development and use in clinical applications.

can generate spectra that distinguishes cholesterol from collagen in coronary plaques through their unique spectroscopic fingerprints [10]. NIRS was first used in 1993 for the detection of lipid content in an experimental animal model [11], followed by subsequent *ex vivo* validation in human cadavers [12]. In 2001, a device prototype for intracoronary imaging was developed, which led to multiple case series and clinical studies in the following decade [13–15]. This technology aims to detect vulnerable lipid-rich plaques (LRPs) by NIRS chemogram [16], whereas recent literature has demonstrated the association of LRP and culprit lesions in ACS [17, 18], as well as with nonculprit lesions in ACS [19], in percutaneous coronary intervention (PCI)-related procedural complications [20, 21], in plaque regression with statins therapy [22] and with the occurrence of cardiovascular events [23]. NIRS received US Food and Drug Administration (FDA) approval for clinical use in 2008 and for NIRS-IVUS system in 2010, followed by regulatory approval in Europe (CE marked) and Japan in 2011 and 2014, respectively (e.g., **Figure 1**) [24].

2. Near-infrared spectroscopy system

2.1. Principles of diffuse reflectance NIRS

Spectroscopy is based on the analysis of electromagnetic spectra induced by near-infrared light and provides direct evaluation of plaque composition, which could yield information on plaque vulnerability [13]. Several spectroscopic methods have been investigated for the purpose of identifying atherosclerotic plaque composition, although the commercially available catheter uses diffuse reflectance NIRS [13, 25]. The principle of NIRS relies on the interaction of light in the form of photons with different functional groups of organic molecules in a tissue, which results in reflected light in the NIR region from molecular vibrational energy in the form of oscillations of atoms within their chemical bonds. Photons can be absorbed or scattered by tissue, which determines the amount of light that is detected by the spectrometer. The wavelengths of light in NIRS are approximately in the 800–2500 nm range. Unique combinations of carbon-hydrogen (C-H), nitrogen-hydrogen (N-H), and oxygen-hydrogen (O-H) bonds are responsible for the major absorption of NIR light, whereas each functional group of large complex molecules yields absorption patterns at specific wavelengths, known as the *spectroscopic chemical fingerprint*, that provides qualitative and quantitative information on sample recognition and tissue characterization (e.g., **Figure 2**) [13, 26, 27].

Diffuse reflectance NIR spectroscopy has many features that enable *in vivo* lipid-core plaques (LCP) analysis in coronary arteries. The term "near" indicates the section of infrared that is closer to the visible light region with a longer wavelength and hence a lower energy than visible light. NIR has the ability to identify organic compounds from light penetration through blood and tissue, since hemoglobin and water have relatively low absorbance in the NIR wavelength, avoiding the need to be in contact with tissue or to clear the field of view with saline or contrast flush or by vessel occlusion [13, 26]. Moreover, it can provide simultaneous image acquisition and nondestructive chemical analysis of biologic tissue with rapid acquisition time (<1 s) from an ultrafast laser source, overcoming cardiac motion artifacts. Diffuse
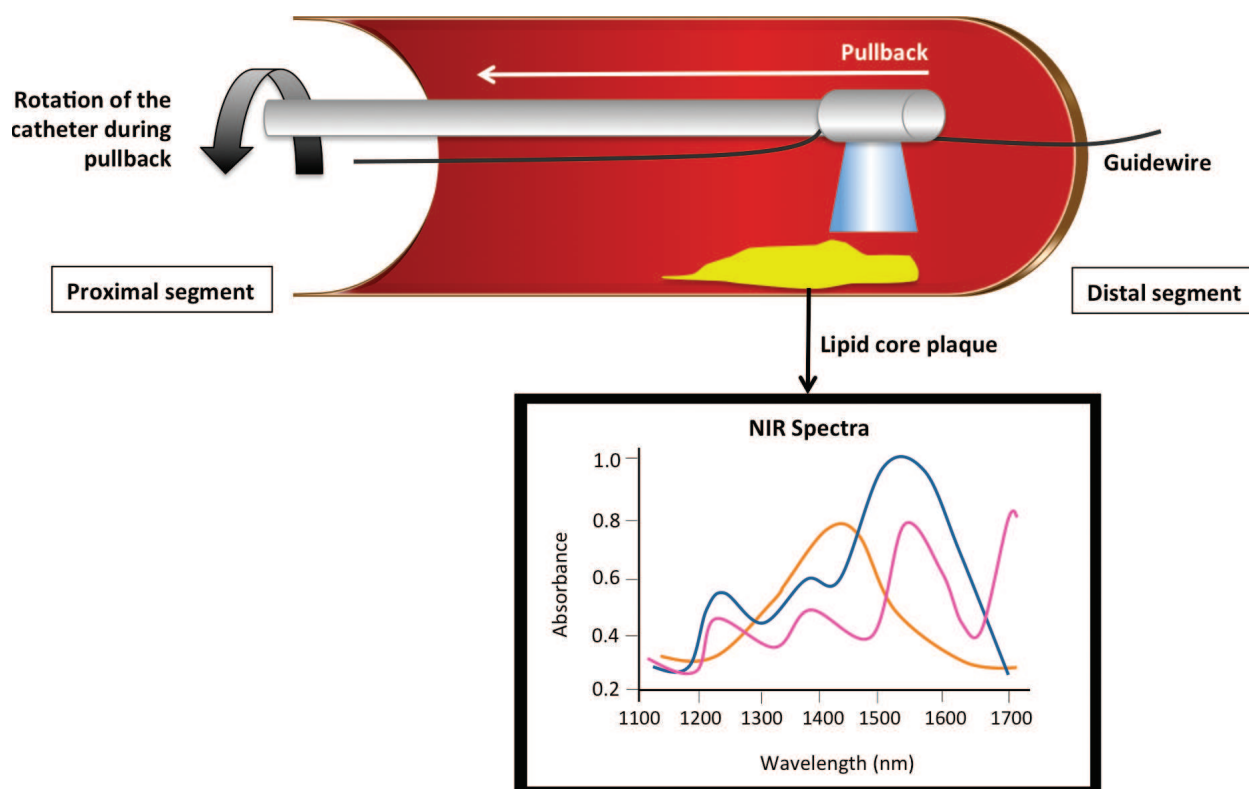
Figure 2. Near-infrared spectra detection and analysis of various components of a lipid-core plaque by NIRS-imaging system. NIRS intracoronary imaging is performed by the catheter's optical tip under automated rotating pullback that enables to rapidly scan the arterial vessel wall circumferentially and longitudinally. The catheter tip emits and collects light that interacts with different functional groups of molecules of the arterial wall and plots the relative absorbance of light across the wavelength range, which generates a spectrum. Thousands of NIR spectra are collected and produces a unique chemical "fingerprint" of the lipid-core plaque.

NIR spectroscopy has been used to identify multiple plasma constituents, to monitor systemic and cerebral oxygenation and also provides a specific chemical measure of LCP [13, 26, 27]. Other spectroscopy techniques are currently under research development for intravascular applications, including Raman spectroscopy, fluorescence spectroscopy, and magnetic resonance spectroscopy (e.g., **Table 1**) [13, 25].

2.2. NIRS-IVUS-combined catheter system

Spectroscopy has a strong fundamental basis for compositional measurement and is a highly efficient method for the identification of chemical components of unknown organic molecules. A single NIRS modality catheter system, the Lipiscan™ (InfraRedx Inc., Burlington, MA, USA), was first developed for invasive detection of LCP [26]. In order to obtain anatomical information on the vessel and optimal plaque characterization, a hybrid technology (TVC Imaging System™, InfraRedx Inc.) combining near-infrared spectroscopy(NIRS) and intravascular imaging (IVUS) was further developed, which allows simultaneous, co-registered acquisition of structural and compositional data of coronary artery plaques. Thus, combining the two complementary technologies enables a complete assessment of patient's arteries, including vessel size and structure, plaque volume, area, and composition [26, 35].

	Raman NIRS	Fluorescence spectroscopy	Diffuse reflectance NIRS	Nuclear magnetic resonance (NMR) spectroscopy
Principle	Raman shift from the scattering of a photon upon interaction with matter, generating a near-infrared wavelength forming the Raman spectra	Absorbance of energy from a tissue exposed to ultraviolet light, which in turns releases energy in the form of light	Reflected light from a tissue detected by the spectrometer at a wavelength, generating a NIR spectrum	Chemical shift from chemical groups exposed to an oscillating electromagnetic field and frequencies decoded by the Fourier transform to generate NMR spectrum
Plaque characterization	Cholesterol esters, collagen, phospholipids, triglycerides, calcium	Collagen, elastin fibers, lipoproteins, calcium, macrophages, foam cells	Lipid-core plaques	Unsaturated and polyunsaturated fatty acids, cholesterol esters, phospholipids, triglycerides
Validation studies	*Ex vivo* and *in vivo* animal and human studies	*In vitro* and *ex vivo* animal and human studies	*Ex vivo* and *in vivo* animal and human studies	13-Carbon NMR used in *ex vivo* and i*n vivo* animal studies
Advantages	Evaluates the chemical composition of living tissues Signal more specific but weaker than diffuse reflectance NIRS (difficult to detect signal *in vivo*)	Strong fluorescence in arterial tissue, enabling rapid time acquisitions	Evaluates the chemical composition of living tissues, NIR light can penetrate blood and acquire signals from structures several millimeters deep relative to tissue surface	Lack of ionizing radiation (less radioactivity with carbon-13), noninvasive modality, enables to study several biological processes with metabolic, physiologic, and anatomic data combined to imaging
Availability	In development— fiber optics catheter-based system for PCI applications under investigation	No *in vivo* applications due to fluorescence signal distortion by hemoglobin	Catheter-based NIRS-IVUS system used as a clinical application	Costly, preclinical research

IVUS: intravascular ultrasound, NIRS: near-infrared spectroscopy; NMR: nuclear magnetic resonance; PCI: percutaneous coronary intervention [13, 28–34].

Table 1. Summary of different spectroscopic methods.

The commercially available NIRS-IVUS imaging system consists of a 3.2-French (F) rapid-exchange catheter compatible with 6F-guiding catheters, a pullback and rotation device, and a console that houses the scanning NIR laser, the computer that processes the spectral signal and two monitors [10, 26, 36]. Within the catheter body is a rotating core of optical fibers that deliver near-infrared light and measure the proportion of light reflected back over the range of optical wavelength (800–2500 nm) in the form of an imaging spectrum. The catheter-imaging core enables to collect data rapidly by rotating at 960 rpm with synchronized pullback

at an automated speed of 0.5 mm/s. The system acquires >30,000 spectra per 100 mm. IVUS images are simultaneously acquired by a transducer at a frequency of 40 MHz and with an axial resolution of 100 μm, together with co-registered NIRS measurements, with a maximum imaging length of 12 cm and a depth of 1 mm or less. Thus, the NIRS spectra data are mapped and paired with corresponding cross-sectional IVUS frames, presented as a ring around the IVUS image [26, 27, 35, 36]. An upgrade version of the TVC catheter Imaging System™ was released by the company in 2015, which uses an extended bandwidth transducer that generates IVUS images at frequencies between 30 and 70 MHz, thus increasing the resolution and depth-to-field of the images [36].

2.3. Interpretation of NIRS data

Upon completion of the automated pullback scan, spectral data are automatically analyzed by a computer-based algorithm that transforms NIR spectra into a probability of LCP presence. The probability is mapped to a color pixel that will generate a digital two-dimensional color map of the artery called the NIRS chemogram, which represents the probability of the presence of LCP over the scanned segment of a vessel (**Figure 3**). On the longitudinal chemogram, the *x*-axis denotes the pullback location (in millimeters) and the *y*-axis represents the circumferential position (degrees of catheter rotation, from 0 to 360°). For each pixel of 0.1-mm length and 1° angle, the lipid-core probability is calculated from the spectral data collected and quantitatively coded on a color scale transitioning from red (0 = low probability of LCP) to yellow (high probability of LCP), with a probability of 0.60. The threshold required for the detection of LCP of interest was defined in the SPECTACL study according to the high prevalence of LCP (58%) detected in scanned segments that met both criteria of spectral adequacy and similarity from 60 patients undergoing PCI for stable CAD or ACS [10]. Pixels with intermediate data, including those that interfere with the guidewire, appear black. The block chemogram is a semi-quantitative summary metric of the probability that an LCP is present in a 2-mm NIRS chemogram segment that is computed and is displayed as a false color map, thus providing a 1:1 direct comparison of the chemogram with histopathology during validation of the lipid prediction algorithm. The blocks correspond to one of four colors (red ($P < 0.57$), orange ($0.57 \leq P < 0.84$), tan ($0.84 \leq P < 0.98$), and yellow ($P \geq 0.98$)), which represents the 90th percentile probability of lipid within the 2-mm segment of the pullback [26, 27, 35, 36]. The 2-mm block chemogram measures were used to compare the NIR spectra to histology in each 2-mm block in a receiver operating characteristic (ROC) curve analysis of diagnostic accuracy, from which LCP probabilities were calculated [10].

Chemometrics is the methodology applied by NIRS technology to analyze lipid content in atherosclerotic arteries [37]. The NIRS system was used in an extensive *ex vivo* study using human coronary arteries autopsy specimens to develop an algorithm for LCP detection. NIR spectra and histological data, used as gold standard, were collected from human autopsy hearts to build a calibration model capable of recognizing the NIR spectral shapes unique to LCP (see Section 2.4.2) [38]. Mathematical models constructed from a calibration set of samples were used to extract and analyze data from NIRS spectra, as reference values for the chemical compounds of interest in the tissue samples were obtained from histopathology samples. Models constructed from these calibration samples correlate the NIRS signals with
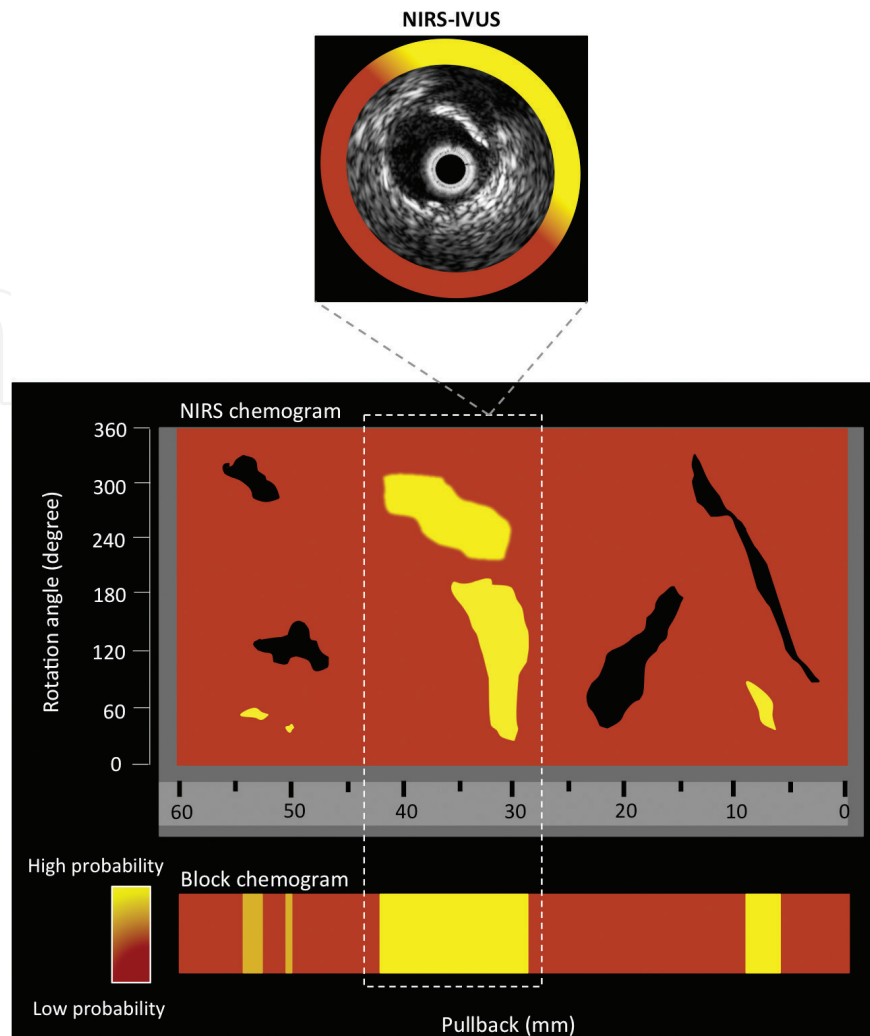
Figure 3. Example of a near-infrared spectroscopy (NIRS) chemogram. The near-infrared spectroscopy chemogram is a digital color-coded map of the arterial wall that is generated from NIR spectra analysis of the arterial wall, which indicates the location and intensity of lipid core in the region of interest (ROI). The *X*-axis represents the pullback position (in mm) and the *Y*-axis indicates the circumferential position of the measurement (in degrees). The block chemogram is a vertical summary of the chemogram at 2-mm pullback intervals. IVUS images are simultaneously acquired and co-registered with NIRS measurements and displayed as cross-section images superimposed with a chemogram.

the reference values, allowing the prediction of future samples on the basis of their NIRS measurements [39, 40]. The algorithm for LCP detection in humans was then prospectively validated in the SPECTACL study, in which chemograms obtained *in vivo* were similar to those obtained in histology controls (see Section 2.4.3) [10].

The lipid-core burden index (LCBI) is a measure of the lipid burden within the scanned region, calculated by dividing the number of yellow pixels that exceed an LCP probability of 0.6 per million by the total number of valid pixels in the segment, then multiplied by a factor of 1000 (LCBI range: 0–1000). Other measures can be computed on the chemogram image, such as the LCBI of a region of interest (ROI) and the maximum LCBI of the 4-mm region within the highest lipid burden within the ROI (maxLCBI$_{4mm}$) [26, 27, 35, 36, 39]. It has been shown that a high

LCBI detected in coronary plaques is associated with an increased risk of future cardiovascular events and periprocedural complications (see Section 2.6), which suggests that LCBI could be a useful biomarker for risk assessment and therapeutic efficacy in future clinical trials.

2.4. Validation of the NIRS-imaging system

2.4.1. Preclinical and autopsy studies

Autopsy, animal, and human studies have been carried out to test the utility and safety of NIRS for the purpose of eventually bringing this technology to patients in the catheterization laboratory. Cassis and Lodder first demonstrated the ability of NIRS to accurately identify low-density lipoprotein (LDL) *ex vivo* in the aorta of hypercholesterolemic rabbits [11, 41]. Furthermore, Jarros et al. [42] demonstrated that the cholesterol content of human aortic samples determined by NIR spectroscopy correlated strongly with that measured by reversed-phase, high-pressure liquid chromatography (correlation coefficient of 0.96). The ability of NIR spectroscopy to detect atherosclerosis in tissue was also demonstrated in human carotid and coronary arteries. Dempsey et al. [27] used diffuse reflectance NIR spectroscopy for the analysis of human carotid plaques exposed at the time of surgery. Transcutaneous NIRS was performed in the operating room during surgical endarterectomy and a NIRS algorithm was developed, using gel electrophoresis as a reference method, to determine lipoprotein composition in carotid specimen from NIR spectra. Their results showed significant near-IR correlation between certain lipoproteins present in carotid plaques and microscopic findings, including microscopic necrosis and ulceration, plaque hemorrhage, and thrombosis. Moreover, these proteins were easily detectable in patients with a medical history of CAD, coronary artery bypass grafting (CABG), and major surgery, and were also correlated with age, sex, and CAD risk factors. Furthermore, Wang et al. [12] reported that *ex vivo* direct measurement of lipid/protein ratios in human carotid atherosclerotic specimens from 25 patients correlated with NIRS spectroscopic findings. Thus, the authors concluded that these ratios could further be used to characterize advanced lesion types with superficial necrotic cores *in vivo* with NIR spectroscopy fitted with a fiber optic probe.

The first study to test the hypothesis that NIR spectroscopy could identify plaque composition and features associated with plaque vulnerability, defined by histology as the presence of lipid pool, thin fibrous cap (<65 μm by ocular micrometry), and inflammatory cell infiltration, was performed in 199 human aortic samples obtained at the time of autopsy [43]. An algorithm was constructed using NIR spectra obtained from 50% of the samples (calibration set) and was then tested on unknown samples (validation set) to determine its ability to identify high-risk features as determined by histology. Spectra associated with each of the three histological features of interest were defined by the results obtained from the calibration set. The main findings of this study were that NIRS could identify histology features associated with plaque vulnerability in human plaques *in vitro*, with a sensitivity and specificity of 90% (35 of 39 lesions) and 93% (56 of 60 lesions) for lipid pool, 77% (13 of 17 lesions) and 93% (76 of 82 lesions) for thin cap, and 84% (37 of 44 lesions) and 91% (49 of 55 lesions) for inflammatory cells, respectively. Moreno

et al. [44] measured the NIRS spectra of 167 sections of fixed coronary artery samples and validated an algorithm against histology for the determination of lipid areas > or <0.6 mm^2, with a sensitivity and a specificity for lipid-rich coronary plaque detection of 83% (5 of 6 lesions) and 94% (60 of 64 lesions), respectively.

Since the intention of inventers of the NIRS system was to commercialize a catheter-based instrument that could assess plaques in coronary arteries *in vivo* and rapidly perform thousands of measurements through blood, Moreno et al. [45] first demonstrated that NIRS could identify lipid-rich plaques *in vivo* through blood in aorta of rabbits with diet-induced atherosclerosis. The catheter NIR spectroscopy was able to identify lipid areas > or <0.75 mm^2 with 78% sensitivity and 75% specificity. Marshik et al. [46] subsequently demonstrated accurate detection by NIRS spectra of lipid-rich plaques from 26 fresh human aorta samples through various amounts of blood up to a depth of 3 mm, with a sensitivity of 88% and a specificity of 79%. Moreover, the performance of the system was evaluated against histology, with favorable results for the detection of thin-cap fibroatheroma (TCFA) and disrupted plaques through blood, thus supporting the development of a NIR catheter for *in vivo* coronary arteries TCFA assessment [47]. To evaluate the performance of the system during cardiac motion, a human coronary autopsy specimen was attached at the surface of a beating pig's heart and connected to the porcine circulation [47]. The prototype 3.2-F NIRS catheter was positioned inside the coronary segment and was able to correctly identify a spectrally distinct target attached to the surface of the graft, despite blood flow and cardiac motion [48, 49].

2.4.2. Autopsy calibration and validation studies

The catheter-based system was improved with the addition of an automated pullback and rotation device allowing the system to circumferentially scan the length of a vessel. Calibration and validation studies of NIRS for the detection of LCP were first performed in human autopsy specimens of coronary arteries [16, 35]. The largest *ex vivo* study, conducted by Gardner et al. [38], aimed to evaluate the ability of the NIRS system to detect LCP in human coronary arteries from 84 autopsied hearts. Coronary arteries, obtained from a broad range of patient characteristics and causes of death, were mounted in a tissue fixture and connected to a blood circulation system with physiologic pressure, temperature, and flow. The resulting set of NIRS spectra and corresponding histology data were used to construct and validate an LCP detection algorithm. A total of 86 coronary segments from 33 hearts were used to calibrate the system algorithm for LCP detection and produced prospectively defined end points. The following 51 hearts and 126 segments were used to validate the accuracy of NIRS in the detection of LCPs in a double-blind, prospective study. In order to develop and validate the algorithm for the identification of LCP in coronary arteries, LCP of interest was defined as a fibroatheroma (FA) containing a lipid core of >0.2-mm thick, with a circumferential span of >60° on cross-section and a mean fibrous cap thickness of <450 μm. Prospective validation of the system for the detection of LCP from 51 hearts yielded an area under the ROC curve (AUC) of 0.80 (95% confidence interval (CI): 0.76–0.85) for average lumen diameters of up to 3.0 mm. The detection of any-sized fibroatheroma in an artery segment using

the LCBI as a measure of lipid burden resulted in an AUC of 0.86 (95% confidence interval (CI): 0.81–0.91). However, false-positive scan results were obtained when the NIRS system was detecting areas with lipid that did not meet criteria of LCP. Moreover, LCPs with extensive calcifications were not detected by NIRS since the near-infrared light cannot penetrate through calcium and other artifacts [22, 38].

2.4.3. Clinical validation studies

The first use of the NIRS system in coronary arteries of living humans was performed in six patients undergoing elective PCI for stable angina using an early prototype (2001; Lahey Clinic, Burlington, MA) [13, 16, 40]. No device-related adverse events occurred, showing the safety and feasibility of the system to distinguish spectra measured through blood. However, significant motion artifacts were present due to slow-signal acquisition time (2.5 s). In August 2005, an improved ultrafast NIR system prototype was developed with a faster scanning laser and was later used in a feasibility study of 10 patients in 2006 (Lahey Clinic, Burlington, MA). The trial confirmed the safety of the newer improved device and showed its ability to discriminate between signals obtained in the artery and those from blood alone, with no measurable artifacts of motion [16, 40].

A subsequent pivotal study, the SPECTACL (SPECTroscopic Assessment of Coronary Lipid) clinical study, was performed to validate the accuracy of LCP-detected NIRS signals collected in coronary arteries of 106 patients [10]. The study met its primary end point of demonstrating that spectral data could be safely acquired in coronary arteries of patients with the intravascular NIRS system and that the spectra were equivalent to those gathered from autopsy specimens (success rate of 0.83; 95% confidence interval (CI): 0.70–0.93). Thus, this study supported the feasibility of LCP detection in living patients. Subsequent studies showed intra- and inter-catheter reproducibility of automated interpretation of NIR spectra signals [50, 51].

2.5. Comparison with other intravascular imaging modalities for plaque characterization

The most common cause of acute coronary syndromes (ACS) is believed to be coronary artery thrombosis due to the rupture of lipid-rich "*vulnerable plaques.*" Thin-cap fibroatheroma (TCFA) plaques, which are characterized by a lipid-laden necrotic core with an overlying thin fibrous cap measuring <65 μm, containing few smooth muscle cells but numerous macrophages, are often the substrate for plaque rupture-induced ACS [3, 4]. TCFAs are associated with positive remodeling and thus predominantly located in areas of the coronary tree that show mild to moderate luminal narrowing [52]. As previously outlined, coronary angiography only detects gross stenotic plaques and provides no insight regarding non-ruptured "*vulnerable plaques,*" which limits plaque burden assessment [6]. Intravascular imaging modalities have been developed to fill part of the gap in information provided by coronary angiography and for *in vivo* detection of LCP [35, 53]. *In vivo* atherosclerotic imaging could enable to detect, predict, and prevent plaque rupture, improve PCI treatment of flow limiting target lesions, and could identify new therapeutic targets that would prevent future adverse coronary events in CAD patients (e.g., **Table 2**).

	Spatial resolution (μm)	Depth (mm)	Energy source	Remodeling	Plaque composition	Calcium	Fibrous cap	Lipid core	Thrombus	Macrophages	Neovessels
IVUS	100–150	10	Ultrasound	++	−	++	±	+	±	−	−
RF-IVUS	100	10	Ultrasound	−	+	++	+	+	−	−	−
OCT	10	2–3	Near-infrared light	−	+	++	++	+	++	+	+
NIRS	1000	−	Near-infrared light	−	−	−	−	++	−	−	−
NIRS-IVUS	100–150	10	Near-infrared light + ultrasound	++	−	++	±	++	±	−	−

IVUS: intravascular ultrasound; NIRS: near-infrared spectroscopy; OCT: optical coherence tomography; RF-IVUS: radiofrequency intravascular ultrasound.

Table 2. A comparison of different intravascular imaging modalities.

2.5.1. Intravascular ultrasound (IVUS) imaging

Intravascular ultrasound imaging (IVUS) produces cross-sectional images of the lumen and the artery wall *in vivo*, enabling visual assessment of plaque echogenicity from axial resolution of approximately 100 μm using high-frequency detectors (up to 45 MHz) [9]. IVUS is very accurate in identifying calcifications (sensitivity and specificity of approximately 90%), plaque burden and, unlike coronary angiography, can detect non-protruding plaques as well as positive and negative vascular remodeling [9, 54]. Thus, IVUS is currently the gold standard for atherosclerotic imaging of the coronary arteries in progression/regression plaque trials [9, 55–57]. In addition to its use as a research tool, IVUS has shown to be of clinical value for the assessment of ambiguous lesions and facilitates optimal PCI procedures by providing reference vessel diameter [9, 58]. A previous study from Lee et al. [59] showed that attenuated lesions on IVUS were more common in ACS patients and were associated with more severe and complex plaque morphology, plaque burden, and higher frequency of no-reflow phenomenon during PCI procedures. Conventional grayscale IVUS has a high sensitivity for detecting lipid deposits (78–95%), visualized as echolucent zones, but a low specificity (30%) [54]. Another limitation of IVUS imaging is the low-axial resolution that does not allow to precisely define thin-cap fibroatheroma (TFCA), whose thickness is usually less than 65 μm in unstable plaques, and thus cannot identify plaques prone to rupture [54].

2.5.2. Virtual histology (VH) imaging

As compared to conventional invasive ultrasound techniques, radiofrequency (RF) IVUS provides additional information on plaque composition and morphology by spectral analysis of ultrasound backscatter [60]. A color-coded map allows the distinction of different components of atherosclerotic plaques, such as calcification (white), lipid/fibrofatty (light-green), fibrous (green) tissue, and necrotic core (red) [61]. Virtual histology (VH)-IVUS spectral analysis correlates with histopathology studies of plaques and can identify the four plaque components with sensitivity, specificity, and predictive accuracy ranging from 80 to 92% [54, 62, 63]. VH-IVUS detection of LCPs has been associated with higher incidence of clinical events [64, 65] and periprocedural complications during PCI [66–68]. Prospective assessment of vulnerable plaques was performed in the PROSPECT (Providing Regional Observations to Study Predictors of Events in the Coronary Tree) trial, a multicenter multimodality study that prospectively analyzed by IVUS and IVUS-VH imaging the coronary arteries of 697 ACS patients [64]. Their findings suggested that the presence of TCFA defined by VH-IVUS (hazard ratio (HR), 3.35; 95% CI, 1.77–6.36; $P < 0.001$), a minimal lumen area of ≤ 4 mm^2 (HR, 3.21; 95% CI, 1.61–6.42; $P = 0.001$), and a large plaque burden of $\geq 70\%$ (HR, 5.03; 95% CI, 2.51–10.11; $P < 0.001$) were independent predictors of major adverse cardiovascular events (MACEs) in nonculprit lesions at 3.4 years follow-up. However, the positive-predictive value was only 18–23%, reflecting MACE's low prevalence. Although this study validated the concept of vulnerable plaque, the lack of specificity and difficulties in image interpretation/measurements prevented these results from changing clinical practice. The VIVA study [65], as well as the PREDICTION [69] and ATHEROREMO-IVUS [70] studies, subsequently reported similar findings, despite differences with the PROSPECT study regarding inclusion criteria, follow-up duration, definitions

of TCFA and MACE. Although RF-IVUS is a validated and promising tool to identify patients and lesions at risk of future ACS, there are limitations regarding axial resolution, accuracy of necrotic core determination, and proper data acquisition and analysis [54, 64, 65].

2.5.3. Optical coherence tomography (OCT)

Optical coherence tomography is an invasive catheter-based imaging modality that measures the intensity and echo time delay of reflected near-infrared light from internal structures in tissues [71]. This technique provides a resolution of 10–20 μm *in vivo*, which is largely superior to IVUS. The recent technology uses the optical frequency domain imaging (OFDI), which enables faster pullback speeds without altering image quality and resolution [9]. The use of non-occlusive techniques with flushing of contrast through the guiding catheter during simultaneous image acquisition has partly resolved the issue of light absorption by blood components. OCT can discriminate features of high-risk plaques by evaluating the lipid content and macrophages infiltration, as well as the measurement of fibrous cap thickness [72]. This imaging modality is also used during percutaneous coronary intervention to assess stent apposition, coronary dissections, neoatherosclerosis and in-stent restenosis, mechanisms of plaque disruption in ACS patients, and more recently to evaluate the scaffold of bioabsorbable stents [73, 74]. The main limitation of OCT is the shallow penetration depth (1.0–2.5 mm) into the tissue, which limits proper imaging of biomarkers in atherosclerotic plaques [9, 75]. Other limitations include the lack of standardization of fibrous cap thickness analysis and the inconsistent accuracy in discriminating lipid-rich plaques from similar optical properties, such as macrophages accumulation, which can lead to false-positive results [72]. Regardless of the limitations, intracoronary FD-OCT remains a promising new clinical method for interrogating the microstructural details of the coronary wall [76].

2.5.4. Near-infrared spectroscopy (NIRS)

In contrast to IVUS, RF-IVUS, and OCT, which collect structural information, NIRS is unique for its ability to directly identify the chemical composition of the arterial wall and assess the presence of the LCP. NIRS detects unequivocal fingerprints from lipid core that is not affected by signal loss behind calcium due to acoustic shadowing, as it can occasionally preclude grayscale IVUS analysis, and the validation of NIRS included both calcified and non-calcified lipid cores in the definition of LCP [38]. NIRS alone does not provide information about structural anatomic parameters, such as vessel remodeling, plaque thickness, lumen area, and calcification [77]. However, as previously mentioned, the combined NIRS-IVUS-imaging catheter allows co-registration of both IVUS and NIRS data, which gives information on both plaque composition and morphology. NIRS-IVUS has shown to improve LCP detection, by comparison to IVUS, in calcified plaques as well as in lesions with small plaque burden [78]. The combined measures of plaque burden and LCBI improved the accuracy of fibroatheroma detection as compared with plaque burden alone by grayscale IVUS. Indeed, Puri et al. [79] conducted an *ex vivo* NIRS and IVUS-imaging study, performed in 116 coronary arteries of 51 autopsied hearts, whereas lesion-based analysis demonstrated that combining plaque burden and LCBI analysis significantly improves fibroatheroma detection accuracy (c index 0.77, $P = 0.028$), by comparison to plaque burden alone.

Several studies have compared NIRS with other intravascular-imaging modalities for LCP detection. It was previously shown that large plaque area measured by grayscale IVUS was more often associated with lipid accumulation/LCP detected by NIRS [19, 80]. However, Brugaletta et al. [80] found a weak correlation between the VH necrotic core content of the plaque and the block chemogram probability values ($r =0.149$), which did not improve after correction for the presence of calcium. In a larger study performed in 131 plaques of 66 vessels, in which 31 plaques (26.7%) were attenuated, the relation between VH-derived percentage necrotic core and NIRS-derived LCBI was not significant ($r = 0.16$, $P = 0.110$) [81]. However, after separation of the plaques according to grayscale IVUS morphology, a positive relationship between VH-derived maximum percentage necrotic core and LCBI was found in non-calcified plaques, but not in calcified plaques. A study conducted in 17 patients who underwent NIRS and OCT imaging showed modest linear correlation between LCBI and maximum lipid arc and lipid index measured by OCT ($r^2 = 0.319$, $P = 0.003$, and $r^2 = 0.404$, $P = 0.001$, respectively) [82]. Furthermore, Roleder et al. [83] conducted a study which aimed to evaluate the accuracy of NIRS-IVUS-imaging modality to detect TCFA in 60 patients with stable CAD, by comparison to OCT used as the gold-standard reference to define TCFA (cap thickness of <65 μm). They showed that OCT-defined TCFA was characterized by positive vessel remodeling with higher lipid-core burden, while NIRS revealed greater LCBI per 2-mm segment ($LCBI_{2mm}$) >315 with a remodeling index >1.046 as a combined criterion value.

In summary, there are important differences in LCP detection between different intravascular-imaging modalities, owing to their different imaging properties and limitations. As previously mentioned, OCT has the highest resolution but the weakest tissue penetration, limiting assessment of plaque burden and overall plaque volume [84]. While IVUS-VH and OCT require image interpretation for the detection of LCP, NIRS provides automated LCP detection without the need for manual imaging processing, facilitating its use in the catheterization laboratory and enabling rapid ad hoc clinical decision making during procedures. Moreover, OCT and NIRS can image through calcified lesions, whereas IVUS cannot. VH-IVUS can incorrectly misclassify intracoronary stents as calcium surrounded by necrotic core, a major limitation that is not found with OCT and NIRS imaging [84]. From the strengths and weaknesses of each individual imaging modality, it appears that the combination of two or more imaging technologies could improve LCP and vulnerable plaque detection [85].

2.6. NIRS-IVUS clinical applications

There is growing evidence from multiple studies of the clinical applications and value of the NIRS-IVUS imaging modality, including identifying the culprit lesion in ACS, optimizing PCI procedure, identifying plaques at high risk of periprocedural complications, for risk stratification, monitoring lipid-lowering therapy, and assessing plaque vulnerability (e.g., **Table 3**) [86].

2.6.1. In vivo detection of culprit lesions in ACS

Several studies have evaluated NIRS detection of LCP, shown by an increased LCBI, at the site of culprit lesions associated with coronary events. Madder et al. [17] performed NIRS imaging in culprit vessels of 20 patients with acute ST-segment elevation myocardial infarc-

Setting	Study or authors	Publishing year	N	Clinical end point(s)	Results, references
LCP detection and *in vivo* validation of NIRS imaging	SPECTACL	2009	106	(1) Evaluate the similarities of NIRS spectra obtained in patients to spectra previously obtained and validated by histology in autopsy specimens; (2) to assess the safety of the device; and (3) to quantify the presence of LCP at target and non-target sites	NIRS system enables to safely obtain spectral data in patients that were similar to those from autopsy specimens and results demonstrated the feasibility of invasive detection of coronary LCP [10]
Plaque characterization	Brugaletta et al.	2011	31	Compare the findings of NIRS, IVUS-VH and IVUS grayscale obtained in matched coronary vessel segments of patients undergoing coronary angiography	Larger plaque area by grayscale IVUS was more often associated with either elevated percentage of VH derived-necrotic core (NC) or LCP by NIRS; correlation between LCP detected by NIRS and NC by VH was weak [80]
	Pu et al.	2012	66	Evaluate NIRS combined with IVUS to provide novel information on human coronary plaque characterization	Combining NIRS and IVUS contributes to plaque characterization *in vivo* [81]
Vulnerable plaque	ATHEROREMO-NIRS	2014	203	Determine the long-term prognostic value of intracoronary NIRS as assessed in a nonculprit vessel in patients with CAD	CAD patients with an LCBI ≥ 43.0 had a fourfold risk of MACE during 1-year follow-up [92]
	Madder et al.	2016	121	Evaluate the association between large lipid-rich plaques (LRP) detected by NIRS at non-stented sites in a target artery and subsequent MACCE	Detection of large LRP by NIRS (maxLCBI$_{4mm}$ ≥400) at non-stented sites in a target vessel was associated with an increased risk of future MACCE [93]
Acute coronary syndrome	Madder et al.	2012	60	Determine the frequency of LCP at target and remote sites in ACS vs. stable angina patients	Target lesions responsible for ACS were frequently composed of LCP; LCP in culprit and non culprit lesions were more common in patients with ACS vs. stable angina patients [77]
	Madder et al.	2013	20	To describe NIRS findings in culprits lesions of STEMI patients	maxLCBI4mm > 400 detected in vivo by NIRS is a threshold for identification of STEMI culprit plaques [17]
	Madder et al.	2015	81	Assess the lipid burden of culprit lesions in NSTEMI and UA patients	LCP similar to those detected at STEMI culprit sites were detected at culprit sites of NSTEMI and UA patients [18]

Setting	Study or authors	Publishing year	N	Clinical end point(s)	Results, references
Periprocedural MI	COLOR registry	2011	62	Analyse the relationship between the presence of large LCP detected by NIRS and periprocedural MI	NIRS provides a rapid and automated detection of extensive LCPs that are associated with a high risk of periprocedural MI [20]
	Raghunathan et al.	2011	30	Evaluate if an association between the presence and extend of LCP detected by NIRS before PCI and periprocedural MI	PCI of LCP detected lesions by NIRS is associated with increased risk of MI after PCI [21]
	Maini et al.	2013	77	Evaluation of LCP modification with coronary revascularization and its correlation with periprocedural MI	Plaque modification can be performed by interventional methods and evaluated with NIRS; axial plaque shifting is an acute prognostic marker for postprocedural MI [124]
PCI optimization	Dixon et al.	2012	69	Compare the target lesions length using NIRS combined with angiography vs. angiography alone	Patients undergoing stent implantation could have LCP extended beyond angiographic margins of the initial target lesion using QCA alone [97]
	Hanson et al.	2015	58	Assess the prevalence of plaque burden and LCP extended beyond angiographic borders of target lesions	NIRS-IVUS imaging demonstrates that target lesion length is commonly underestimated by angiography alone [98]
	Ali et al.	2013	65	Characterize neointimal composition of in-stent restenosis in both BMS and DES using a multimodality approach with OCT and NIRS-IVUS	In-stent thin-cap neoatherosclerosis is more prevalent, more diffusely distributed across stented segment and is associated with increased periprocedural MI in DES compared with BMS [108]
	Madder et al.	2016	120	Evaluate NIRS-IVUS system findings of increased lipid signals in pre-existing stents, speculated to indicate neoatherosclerosis, and compare with a control group of freshly implanted stents, in which any lipid signal originates from fibroatheroma under the stent	Detection of LCP in pre-existing stents by NIRS alone is not reliable evidence of neoatherosclerosis, as the lipid signal may originate from fibroatheroma under the stent [109]
Monitoring lipid-lowering therapies	YELLOW	2013	87	Determine the impact of short-term intensive statin therapy (Rosuvastatin 40 mg OD) on intracoronary plaque content	Short-term intensive treatment with statin was associated with a significant reduction in LCBI / lipid content compared to standard therapy [22]

Setting	Study or authors	Publishing year	N	Clinical end point(s)	Results, references
Prevention of PCI complications	Brilakis et al.	2012	9	Investigate whether the use of a distal embolic protection device might prevent complications of LCP interventions	The use of a distal protection device frequently resulted in embolized material retrieval after stenting of native coronary artery lesions with large LCP [123]
	CANARY	2015	85	Evaluate if a distal protection device reduce postprocedural MI for PCI of LCP lesions	Distal protection device dis not reduce postprocedural MI [125]
	Erlinge et al.	2015	18	Evaluate if aspiration thrombectomy reduces the lipid content of culprit plaques by NIRS-IVUS in ACS patients assessed	Thrombus aspiration resulted in a 28% reduction in lipid content by performing aspiration thrombectomy in culprit lesion [129]

ACS: acute coronary syndrome; BMS: bare-metal stent; CAD: coronary artery disease; DES: drug-eluting stent; IVUS: intravascular ultrasound; LCBI: lipid-core burden index; LCP: lipid-core plaque; LRP: lipid-rich plaque; MACE: major adverse cardiac events; MACCE: major adverse cardiac and cerebrovascular events; MI: myocardial infarction; NC: necrotic core; NIRS; near-infrared spectroscopy; NSTEMI: non-ST-segment elevation myocardial infarction OCT: optical coherence tomography; PCI: percutaneous coronary intervention; QCA: quantitative coronary angiography; STEMI: ST-segment elevation myocardial infarction; UA: unstable angina; VH: virtual histology.

Table 3. A summary of intracoronary human NIRS clinical studies to identify lipid-core plaques (LCPs).

tion (STEMI) and compared their findings with spectra analysis in nonculprit segments of the artery and with autopsy control segments. The maxLCBI$_{4mm}$ was 5.8-fold higher in STEMI culprit segments than in 87 nonculprit segments of the STEMI culprit vessel (median (interquartile range (IQR)): 523 [445 to 821] vs. 90 [6 to 265]; $P < 0.001$). Moreover, maxLCBI$_{4mm}$ was 87-fold higher than in 279 coronary autopsy segments free of large LCP by histology (median (interquartile range (IQR)): 523 [445 to 821] vs. 6 [0 to 88]; $P < 0.001$). Thus, a threshold of maxLCBI$_{4mm}$ ≥400 distinguished STEMI culprit segments *in vivo* from coronary artery autopsy segments free of LCP with high accuracy (sensitivity: 85%; specificity: 98%) [17]. Among the first 85 STEMI cases, two patients showed culprit lesions that did not contain lipid plaque, but rather a calcified nodule in one case and a coronary dissection in the other [15].

Similar NIRS findings of lipid burden were observed in culprit lesions of patients in non-ST segment elevation myocardial infarction (NSTEMI) [18, 77]. LCPs are more common in patients with ACS compared to stable angina patients. From the 81 NSTEMI and unstable angina (UA) patients who underwent culprit vessel NIRS imaging prior to stenting, non-STEMI culprit segments had a 3.4-fold greater maxLCBI$_{4mm}$ than nonculprit segments (448 ± 229 vs. 132 ± 154, $P < 0.001$) and unstable segments had a 2.6-fold higher maxLCBI$_{4mm}$ than nonculprit lesions (381 ± 239 vs. 146 ± 175, $P < 0.001$) [18]. Culprit segments in NSTEMI patients were more often characterized by a maxLCBI$_{4mm}$ ≥400 than those with UA, with a sensitivity of 63.6% versus 38.5%, respectively. Moreover, a large LCP was identified by NIRS within the culprit lesions of five cases of resuscitated out-of-hospital cardiac arrest that subsequently underwent coronary angiography [87]. There is a stepwise increase in lipid content, represented by maxLCBI$_{4mm}$, from nonculprit lesions (0–130), to unstable angina (≈380), to NSTEMI (≈450) and STEMI patients (≈550), supporting the concept of more fibrotic lesions in stable angina and more lipid-rich vulnerable plaque in STEMI, NSTEMI, and sudden death [15]. NIRS-IVUS evidence of LCP with a large plaque burden suggests that the lesion is a culprit, and that such information could be relevant in patients with ambiguous coronary angiography for efficient treatment management.

2.6.2. Association with cardiovascular risk factors

A recent clinical study has evaluated the association between clinical risk factors and blood characteristics of vascular inflammation and lipid content/LCP visualized by NIRS. de Boer et al. [19] reported the use of NIRS in a nonculprit coronary artery in 208 patients undergoing percutaneous coronary intervention or invasive diagnostic coronary exploration for various indications. It was found that male gender, hypercholesterolemia, and the presence of multivessel CAD were modestly associated with higher LCBI values on NIRS. A history of peripheral vascular disease and/or cerebral disease and the use of beta-blockers were positively associated with LCBI, while biomarkers such as blood lipids and high-sensitivity C-reactive protein were not. All clinical characteristics reflecting patients with high CAD risk explained only 23% of the variability in LCBI. Moreover, the LCBI on NIRS and the percentage area of plaque burden determined by IVUS were modestly correlated (r =0.29). In the light of these results, this study could not address the prognosis value of NIRS-imaging modality. Methodological caveats could in part explain the low correlation obtained between NIRS and

IVUS imaging, including the use of lower-frequency IVUS catheters (20 MHz), IVUS and NIRS acquisitions performed using different catheters, measurement of a single cross section on IVUS, and the absence of data regarding the reproducibility of repeated NIRS pullbacks and measurements [88].

2.6.3. Assessing plaque vulnerability and risk stratification

Retrospective autopsy studies have revealed specific histological culprit lesion morphologies in patients suffering from an ACS, which has created an enthusiasm in the use of intravascular coronary artery imaging in search of the "*vulnerable plaque*" at risk of rupture and endoluminal thrombosis. The thin-cap fibroatheroma (TCFA) is believed to be the precursor lesion of plaque rupture, although there is a lack of prospective robust evidence in the literature [15, 89]. A prospective animal study conducted in an atherosclerotic and diabetic pig model showed that NIRS-IVUS imaging can detect and predict the future development of inflamed fibroatheromas with subsequent validation against postmortem histology [90]. The features of rupture-prone plaques included thinned fibrous cap, increased plaque and necrotic core areas, increased concentration of activated inflammatory cells, and the presence of apoptotic and proliferating cells within the fibrous cap [90]. An autopsy study of 103 coronary arteries from 56 autopsied hearts, aiming to assess grayscale IVUS and NIRS detection of histological fibroatheroma (FA), with histology validation as the gold standard, showed that both superficial IVUS attenuation and NIRS-LCP had a similar high specificity of approximately 95% in detecting FAs, however IVUS showed a low sensitivity (36% vs. 47%; P =001) [91]. The addition of NIRS significantly increased the accuracy of fibroatheroma detection at the minimum lumen area from 75% to 89% among all cross-sections ($P < 0.05$). When either IVUS attenuation or lipid-rich plaque was present, the sensitivity for prediction of an FA was significantly higher compared with IVUS alone (63% vs. 36%, $P < 0.001$) and NIRS alone (84% vs. 65%, $P < 0.001$).

The first prospective human study, published in 2014, has evaluated the association of high LCP by NIRS and cardiovascular events. The ATHEROREMO-NIRS (The European Collaborative Project on Inflammation and Vascular Wall Remodeling in Atherosclerosis—Near-Infrared Spectroscopy) trial is a prospective, observational study that aimed to evaluate the prognostic value of NIRS in a nonculprit coronary artery from 203 patients referred for angiography due to stable angina or ACS [92]. The results showed that the 1-year cumulative incidence of all-cause mortality, non-fatal ACS, stroke, and unplanned coronary revascularization was 4-fold increased in patients with an LCBI equal or above to the median value of 43.0 compared to those with an LCBI value below the median (adjusted HR: 4.04; 95% CI: 1.33–12.29; $P = 0.01$). The association of the LCBI value with primary end point was similar in both stable and ACS patients. Although these results are promising, the number of events in this trial was small, and therefore studies with larger number of events will be required for the validation of vulnerable patient detection with NIRS-IVUS imaging. A more recent NIRS-IVUS single-center registry study was conducted in 121 consecutive patients undergoing combined NIRS and IVUS imaging to evaluate the association of large lipid-rich plaques at non-stented sites in a target vessel and subsequent major adverse cardiovascular and cere-

brovascular events (MACCE) [93]. The results showed that the presence of large LCP in a non-stented segment, defined by NIRS maxLCBI$_{4mm}$ ≥400 at baseline, was associated with a significantly increased risk of future MACCE during follow-up (HR 10.2, 95% CI: 3.4–30.6; $P < 0.001$). This study, although single center, underpowered, and with limited follow-up, was consistent with the findings of ATHEROREMO-NIRS study, whereas NIRS detection of lipid burden was associated with patient-level risk of future MACCE [93].

The detection of fibroatheroma could help to identify culprit lesions in ACS patients, predict lesions subject to periprocedural complications, could allow optimal stent selection, and reduce the rate of stent restenosis. Whether the detection of fibroatheroma using NIRS-IVUS will prevent future events is currently being studied in several trials, including the Lipid-Rich Plaque study (LCP; Clinical Trials.org Identifier: NCT02033694), PROSPECT II ABSORB trial (A Multicentre Prospective Natural History Study Using Multimodality Imaging in Patients With acute Coronary Syndromes; Clinical Trials.org Identifier: NCT02171065), and ORACLE-NIRS trial (Lipid cORe Plaque Association With CLinical Events: a Near-InfraRed Spectroscopy Study; Clinical Trials.org Identifier: NCT02265146).

2.6.4. Optimizing percutaneous coronary intervention procedures

Visual estimation of a coronary stenosis on a two-dimensional (2D) angiography or quantitative coronary angiography (QCA) of lesion lengths is often misleading from image foreshortening and underestimation of plaque burden. IVUS offers accurate length measurement during automated pullback, proximal and distal reference diameter of a vessel, and enables to evaluate the presence and extent of calcifications [26]. The ADAPT-DES (Assessment of Dual Antiplatelet Therapy With Drug-Eluting Stents) study, a prospective, multicenter, nonrandomized "all-comers" registry of 8583 consecutive patients, showed that IVUS-guidance PCI, performed in 39% of patients, was associated with reduced 1-year rates of MACE (3.1% vs. 4.7%; adjusted HR, 0.70; 95% CI: 0.55–0.88; P = 002), as compared to angiography guidance alone [94]. The benefits of IVUS were observed in patients with ACS and complex lesions, although significant reductions in MACE were present in all patient subgroups, including stable angina and single-vessel disease. Similar results were observed in subsequent meta-analysis [95, 96].

The use of combined NIRS-IVUS imaging may further optimize stent implantation by accurate identification of lipid margins, and thus cover all the segments with high lipid burden. Dixon et al. [97] analyzed 75 lesions with NIRS imaging and demonstrated that lipid-core plaque extended beyond the angiographic margins of the initial target lesion in 16% of cases. Hanson et al. [98] showed that atheroma, defined as plaque burden >40% or LCP, extended beyond angiographic margins in 52 of the 58 lesions analyzed with NIRS-IVUS (90% of lesions), with a mean lesion length that was significantly longer when assessed by NIRS-IVUS as compared with angiography alone (19.8 ± 7.0 vs. 13.4 ± 5.9 mm; $P < 0.0001$). Those results suggests that NIRS-IVUS guidance during PCI procedures, as a "red-to-red" stenting strategy, could optimize complete LCP coverage by a stent with the proper length according to the landing zones and thus reduce the risk of edge dissections, stent failure, and subsequent adverse clinical outcomes [26, 39, 99–101]. Although it seems rationale to implant the edges of a stent in a normal artery segment, the marginal increased risk of stent thrombosis and restenosis with

longer stents will require future studies to determine if routine use of NIRS-IVUS for proper stent sizing will improve patient outcomes [102].

Detection of lipid core in a lesion has also been used as one of the factors to consider in the decision to implant a bare metal stent (BMS) or a drug-eluting stent (DES). Several studies have demonstrated a greater frequency of stent thrombosis after DES implantation when struts were penetrating into a lipid-rich necrotic core plaque rather than in a non-yellow (fibrous) plaque [103, 104]. The absence of struts coverage by the formation of a neointima layer during vessel's healing process was seen with both DES and BMS implantation in lipid-rich plaques, which is likely the underlying mechanism of stent thrombosis seen in those patients [105, 106]. Neoatherosclerosis is an important contributor to late-stent thrombosis with newer generation DES, as well as late in-stent restenosis. Histologically, neoatherosclerosis is characterized by the accumulation of lipid-laden macrophages within the neointima with or without necrotic core formation and/or calcification and can occur months to years following stent placement [107]. Originally described in postmortem studies, neoatherosclerosis has more recently been detected by intracoronary imaging. Ali et al. [108] used NIRS and OCT to assess the development of neoatherosclerosis in 65 consecutive patients with symptomatic in-stent restenosis. The prevalence of LCP within neointimal hyperplasia segments was 89% using NIRS versus 62% using OCT. Neoatherosclerosis was associated with significantly reduced minimal cap thickness with plaque rupture occurring exclusively in those patients. Moreover, DES had a higher prevalence and earlier occurrence of neoatherosclerosis, thinner cap, and more lipid burden and density. However, LCP identified by NIRS alone was not associated with periprocedural MI during treatment for in-stent restenosis, which reflects the limited ability of NIRS to differentiate lipid located within the neointimal tissue from a lipid core located underneath stent struts. Nevertheless, postmortem imaging and subsequent histology analysis showed that NIRS could correctly characterize lipid despite the presence of metal struts. Similar findings were reported in a study published by Madder et al. [109], whereas NIRS was not reliable for neoatherosclerosis detection when used as the sole imaging modality for LCP detection. The NIRS lipid signal could not distinguish neoatherosclerosis from fibroatheroma underlying the stent. No doubt that NIRS can detect coronary LCP, but it seems unlikely suitable as a standalone technique for accurate neoatherosclerosis detection and that the adjunction of IVUS or OCT will be required to determine the position of NIRS lipid signal relative to the underlying stent struts [110].

It was proposed that the growth of neointima tissue on the top of a vulnerable plaque might increase the thickness of the fibrous cap [103, 110, 111]. Brugaletta et al. [112] reported the ability of bioresorbable vascular scaffold (BVS) implantation to promote the growth of neointimal tissue, which acts as a barrier to isolate vulnerable plaques. An ongoing trial, the PROSPECT II ABSORB sub-study trial (Clinical Trials.org Identifier: NCT021711065), will randomize patients with plaques at high risk of causing future coronary events (plaque burden ≥70%) to receive an Absorb™ BVS (Abbott Vascular, IL, USA) with optimal medical therapy (OMT) versus OMT alone. This sub-study aims to evaluate the changes in the plaque at 2 years follow-up. Clinically, large LCPs have been shown to be associated with MACE, especially periprocedural myocardial infarction [21]. Whether lipid burden influences long-term outcomes following stent implantation remains elusive.

2.6.5. Prevention of periprocedural complications

Approximately 3–15% of percutaneous coronary interventions are complicated by periprocedural myocardial infarction (PPMI) and no-reflow, in part by distal embolization of intraluminal thrombus and/or lipid-core plaque content, which is associated with adverse long-term outcomes [113, 114]. It was reported that periprocedural MIs are associated with increased atherosclerotic burden and large LCPs [115–118]. Indeed, embolization of the lipid core after stent implantation in a plaque with high lipid content has been identified as an important cause of periprocedural no-reflow and MI with and without the presence of intracoronary thrombus [118–120]. A pilot study performed in nine patients using an embolic protection device showed that embolized material consisted in fibrin and platelet aggregates, which reflects the highly thrombogenic content of necrotic core of large atheroma plaques and LCP [98, 120, 121]. In a sub-study of the COLOR (Chemometric Observation of Lipid-Core Plaques of Interest in Native Coronary Arteries) registry, a prospective multicenter observational study aiming to determine a relationship between NIRS-defined high LCBI and periprocedural MI, Goldstein et al. [20] analyzed the cardiac biomarkers of 62 stable patients undergoing PCI. The main findings were that periprocedural MI, defined in the study as a postprocedural elevation above three times the upper limit of normal (ULN) for either creatine kinase-MB (CK-MB) or cTnI measured 4–24 h after PCI, occurred in nine patients (14.5%) and was more common among patients with a $maxLCBI_{4mm} \geq 500$ (7 of 14 patients, 50%) versus patients with a $maxLCBI_{4mm} < 500$ (2 of 48 patients, 4.2%). The authors concluded that a high LCP, defined as a $maxLCBI_{4mm} \geq 500$, was associated with periprocedural events. These results are concordant with the registry study conducted by Raghunathan et al. [21], in which the analysis of 30 patients who underwent pre-procedure NIRS imaging showed a postprocedural increase of CK-MB more than three times the UNL in 27% of patients with a ≥1 yellow blocks (n = 11) as opposed to none in the 19 patients without a yellow block within the stented lesion.

Distal embolization, as an important mechanism of periprocedural MI, was further supported by several studies that have demonstrated a significant decrease in the size of LCP after stenting [122–124]. Stone et al. showed in the CANARY trial that LCP measured as LCBI by NIRS in the stented vessels reduces with PCI treatment, with a significant reduction of median LCBI from 143.2 before PCI to 17.9 after PCI ($P < 0.001$) [125]. Moreover, the authors showed that the occurrence of periprocedural MI was associated with higher LCBI, results that are concordant with previous findings [20, 21].

In order to prevent periprocedural MI during PCI, several strategies were proposed during stenting procedures, including aspiration thrombectomy, embolization distal-protection devices, vasodilators, intensive anticoagulation, and antiplatelet therapies. The CANARY (Coronary Assessment by NIR of Atherosclerotic Rupture-Prone Yellow) trial randomized 85 stable angina patients undergoing stent implantation of a single native coronary lesion and pre-procedure NIRS-defined $maxLCBI_{4mm} \geq 600$ to PCI with or without distal-protection filter [125]. Among the 31 randomized cases with a $maxLCBI_{4mm} \geq 600$, there was no difference in the rates of periprocedural MI with or without the use of distal-protection filter (35.7 vs. 23.5%, respectively; relative risk 1.52; 95% CI: 0.50–4.60, P =0.69). It should be noted that the CANARY trial was ended prematurely due to difficulties in identifying patients suitable

for randomization to embolic-protection devices and lack of signs of benefits and thus was not adequately powered to detect a difference in MI or other major procedural complications between the two patient groups. An ongoing study, the CONCERTO (Randomized-Controlled Trial of a Combined versus Conventional Percutaneous Intervention for Near-Infrared Spectroscopy Defined High-Risk Native Coronary Artery Lesions; Clinical Trials.org Identifier: NCT02601664) trial, aims to evaluate different strategies for periprocedural MI prevention. Patients undergoing PCI with high-risk native coronary lesion, defined as ≥2 contiguous yellow blocks on the block chemogram, are randomized to combined preventive measures versus conventional PCI. The combined preventive measures consist of pre-PCI administration of an intracoronary vasodilator and a glycoprotein IIb/IIIa inhibitor, in addition to the use of an embolic-protection device if technically feasible and a complete coverage of the LCP if technically feasible.

Thrombectomy is often used to aspirate thrombus and restore blood flow in the culprit vessel during primary PCI in STEMI patients. The clinical benefits of routine thrombus aspiration remain a matter of debate, since the TAPAS (Thrombus Aspiration during Percutaneous Coronary Intervention in Acute Myocardial Infarction) study demonstrated a reduction of mortality while larger studies such as TASTE (Thrombus Aspiration in ST-Elevation Myocardial Infarction in Scandinavia) and TOTAL (Trial of Routine Aspiration Thrombectomy with PCI versus PCI Alone in Patients with STEMI) did not show a reduction of cardiovascular mortality, with an increased rate of stroke at a 30-day follow-up in the TOTAL trial [126–128]. Erlinge et al. [129] performed NIRS-IVUS imaging in 18 ACS patients to examine if aspiration thrombectomy reduced the lipid content of ACS culprit plaques. The culprit lipid content was quantified by NIRS-IVUS before and after thrombectomy as the lipid-core burden index (LCBI), and aspirates were examined by histological staining for lipids, calcium, and macrophages. Culprit lesions were found to have high lipid content prior to thrombectomy, which resulted in a 28% reduction in culprit lesion lipid content (pre-aspiration LCBI 466 ± 141 vs. post-aspiration 335 ± 117, $P = 0.0001$).

As aforementioned, the use of intracoronary NIRS-IVUS imaging for accurate identification of LCP lesions prone to embolize, as well as different treatment strategies, for periprocedural MI prevention are attractive approaches, however their clinical benefits on myocardial salvage and prevention of embolization remains to be demonstrated in future studies.

2.6.6. Monitoring effects of lipid-lowering therapies

It is well known that statin therapy reduces rates of cardiovascular events in secondary prevention. The pharmacological effects of specific lipid-reducing agents that reduce free and esterified cholesterol could be evaluated with NIRS, as it informs on the lipid content of coronary artery plaques over time. The demonstration of markedly reduced LCBI values in a patient after 1 year of high-dose rosuvastatin therapy was the first indication that NIRS-IVUS could be used to evaluate the effect of systemic anti-atherosclerotic medical therapy [130]. In the YELLOW (Reduction in Yellow Plaque by Aggressive Lipid-Lowering Therapy) trial, Kini et al. [22] prospectively randomized 87 patients with multivessel coronary artery disease undergoing PCI with one culprit and one nonculprit hemodynamically significant

lesions, defined by fractional flow reserve (FFR <0.80), to receive intensive statin therapy (rosuvastatin of 40 mg daily) or standard lipid-lowering therapy. The nonculprit lesions had a baseline assessment by NIRS-IVUS and FFR, prior to randomization. Rosuvastatin therapy resulted in a significant reduction in the plaque lipid content/maxLCBI$_{4mm}$ compared to standard therapy. The significant reduction in maxLCBI$_{4mm}$ associated with intensive statin therapy was observed across subgroups of the study population, based on age, gender, presence of diabetes, and baseline lipid profile. However, no significant changes were observed for the maxLCBI$_{4mm}$ and LCBI measurements at the lesion site in the standard lipid treatment group at follow-up. Although baseline LCBI was significantly higher in patients randomly allocated to intensive versus standard therapy, the YELLOW trial highlights that LCP measured by NIRS was associated with CAD and that it could be a potential tool to monitor regression of the disease in phase II clinical trials evaluating novel anti-atheromatous therapies.

A similar study of the effect of rosuvastatin treatment on the coronary plaque composition and necrotic core, the IBIS-3 (Integrated Biomarker and Imaging Study 3) trial, failed to demonstrate a significant reduction of necrotic core volume or LCBI under intensive rosuvastatin therapy for 1 year [131]. The effects of high-dose statin therapy are being further investigated in the YELLLOW II trial (Clinical Trials.org Identifier: NCT01837823), a phase II clinical study, that aims to assess the regression of plaque lipid content and changes in plaque morphology from atherosclerotic lesions after 8–12 weeks of high-dose statin therapy by utilizing NIRS, IVUS, and OCT imaging modalities in the coronary arteries.

2.7. Limitations of the technology

Near-infrared spectroscopy (NIRS) identifies the chemical signature of the lipid component, specifically lipid core-containing coronary plaque (LCP). The main limitations of NIRS technology are the lack of information regarding the lumen, plaque anatomy, and status of the fibrous cap or its attenuation. Although NIRS may be one of the most sensitive modalities to detect lipid-core plaques, it cannot provide information on the depth of the lipid core. Moreover, the accurate measurement of lipid volume/burden with NIRS has not been validated [132]. To overcome these pitfalls, a new combined imaging catheter adding intravascular ultrasound (IVUS) imaging was developed. However, since intravascular ultrasound has a low sensitivity to visualize lipid inside a plaque, the additional value of this new system will require further evaluation [26].

The clinical relevance of imaging specific features of the vulnerable plaque for risk stratification and clinical decision making remains unclear. Higher-resolution imaging modalities, such as OCT, better assessed determinants of vulnerable plaques than NIRS; however, there is currently no commercialized system combining OCT and NIRS modalities. The prognostic utility and incremental value of NIRS when associated with biomarkers of plaque vulnerability assessed by IVUS (plaque burden, MLA, and remodeling) remains to be investigated [26, 133]. Many studies have brought evidence that IVUS-guided PCI achieves superior outcomes compared to angiography guidance alone [134]. The potential value of adding NIRS for lipid-rich plaques at risk of embolization and for a complete coverage of LCPs remains to be investigated.

NIRS-IVUS-imaging modality is an invasive diagnostic modality that targets patients in the setting of secondary prevention, thus precluding its utilization for primary prevention, along with other invasive imaging technologies.

2.8. Future trials and perspective

NIRS-IVUS-imaging technology is improving and should become a sensitive modality for coronary plaque characterization. A new algorithm for collagen detection has been developed using the same spectroscopy signal, which enables to detect the amount of fibrous tissue over the LCP (thin or thick fibrous cap) [15]. This technology will be further optimized by adding a recently developed, but not yet available, high-resolution IVUS, which will allow to accurately differentiate between thin and thick fibrous caps. Co-registration of NIRS with other imaging modalities is also being developed. The use of combined OCT-NIRS catheters has been recently demonstrated as a proof of concept [15].

NIRS-IVUS has also been used in the carotid arteries to detect LCP, which could represent a suitable imaging modality to determine the risk of stroke or the risk of complications during carotid stent placement or endarterectomy. However, this new clinical application remains to be validated in future studies [15].

Multiple prospective outcome studies are currently ongoing to evaluate the ability of NIRS-IVUS imaging to detect vulnerable plaques that are likely to cause future adverse events. Among those studies are the LRP trial (Lipid-rich Plaque Study; Clinical Trial.org Identifier: NCT02033694), the PROSPECT II ABSORB trial (Providing Regional Observations to Study Predictors of Events in the Coronary Tree II; Clinical Trial.org Identifier: NCT02171065), and the ORACLE-NIRS trial (Lipid-core plaque association with clinical events: a near-infrared spectroscopy study; Clinical Trial.org Identifier: NCT02265146). The YELLOW II trial (NCT01837823), which aims to evaluate the effects of rosuvastatin treatment on lipid content after 8–10 weeks of treatment regimen, has completed patient enrolment but results are still pending. Another trial has been completed and awaiting for results publication, the NIRS-TICAGRELOR trial (Clinical Trial.org Identifier: NCT02282332), which aims to evaluate the effect of the P2Y12 inhibitor ticagrelor (AstraZeneca, Cambridge, England) on plaque stabilization and reduction of inflammation by NIRS-defined reduction of LCBI in patients on long-term statin therapy undergoing non-urgent PCI.

3. Conclusion

NIRS is a promising tool for the detection of vulnerable plaques in CAD patients, PCI-guidance procedures, and assessment of lipid-lowering therapies. NIRS-IVUS has been shown to be a reliable and reproducible modality for the detection of intracoronary LCPs, with validation using the current gold-standard, histology. It has already been shown that this imaging modality is highly specific for identifying NSTEMI and STEMI culprit plaques, that it can be used to follow the progression of vulnerable plaques over time, and to evaluate the effect of lipid-lowering therapies and intracoronary devices. Moreover, preliminary data have shown

that NIRS-IVUS-imaging technology can identify vulnerable patients. Multiple ongoing clinical trials will hopefully validate this tool for vulnerable plaque and patient detection, as well as for treatment management and follow-up of patients with CAD.

Abbreviations

ACS	Acute coronary syndrome
BMS	Bare-metal stent
BVS	Bioresorbable vascular scaffold
CAD	Coronary artery disease
CABG	Coronary artery bypass graft
CCA	Conventional coronary angiography
CK-MB	Creatine kinase-MB
cTnI	Cardiac troponin I
DES	Drug-eluting stent
Fr	French
FA	Fibroatheroma
FDA	US Food and Drug Administration
FD-OCT	Frequency-domain optical coherence tomography
FFR	Fractional flow reserve
IVUS	Intravascular ultrasound
LCBI	Lipid-core burden index
LCP	Lipid-core plaque
LDL	Low-density lipoprotein
LRP	Lipid-rich plaque
MACE	Major adverse cardiac events
MACCE	Major adverse cardiac and cerebrovascular events
$maxLCBI_{4mm}$	Maximum lipid-core burden index in 4-mm region
MI	Myocardial infarction
MLA	Minimal lumen area
NC	Necrotic core
NIRS	Near-infrared spectroscopy

NSTEMI	Non-ST segment elevation myocardial infarction
OCT	Optical coherence tomography
OFDI	Optical frequency domain imaging
OMT	Optimal medical therapy
PCI	Percutaneous coronary intervention
PPMI	Periprocedural myocardial infarction
QCA	Quantitative coronary angiography
ROI	Region of interest
SCD	Sudden cardiac death
STEMI	ST-segment elevation myocardial infarction
TCFA	Thin-cap fibroatheroma
UA	Unstable angina
ULN	Upper limit of normal
VH	Virtual histology

Author details

Marie-Jeanne Bertrand[1,2], Philippe Lavoie-L'Allier[1,2] and Jean-Claude Tardif[1,2]*

*Address all correspondence to: jean-claude.tardif@icm-mhi.org

1 Montreal Heart Institute, Montreal, Canada

2 Faculty of Medicine, Université de Montréal, Montreal, Canada

References

[1] White HD, Chew DP. Acute myocardial infarction. Lancet. 2008;372:570–584. DOI: 10.1016/S0140-6736(08)61237-4

[2] Bentzon JF, Otsuka F, Virmani R, Falk E. Mechanisms of plaque formation and rupture. Circ Res. 2014;114:1852–66. DOI: 10.1161/CIRCRESAHA.114.302721

[3] Muller JE, Tofler GH, Stone PH. Circadian variation and triggers of onset of acute cardiovascular disease. Circulation. 1989;79:733–743. DOI: 10.1161/01.CIR.79.4.733

[4] Virmani R, Kolodgie FD, Burke AP, Farb A, Schwartz SM. Lessons from sudden coronary death: a comprehensive morphological classification scheme for atherosclerotic lesions. Arterioscler Thromb Vasc Biol. 2000;20:1262–1275. DOI: 10.1161/01.ATV.20.5.1262

[5]   Chamuleau SA, van Eck-Smit BL, Meuwissen M, Piek JJ. Adequate patient selection for coronary revascularization: an overview of current methods used in daily clinical practice. Int J Cardiovasc Imaging 2002;18:5–15. DOI: 10.1023/A:1014372125457

[6]   Mintz GS, Painter JA, Pichard AD, Kent KM, Satler LF, Popma JJ, Chuang YC, Bucher TA, Sokolowicz LE, Leon MB. Atherosclerosis in angiographically "normal" coronary artery reference segments: an intravascular ultrasound study with clinical correlations. J Am Coll Cardiol. 1995;25:1479–1485. DOI: 10.1016/0735-1097(95)00088-L

[7]   Glagov S, Weisenberg E, Zarins C, Stankunavicius R, Kolletis G. Compensatory enlargement of human atherosclerotic coronary arteries. N Engl J Med. 1987;316:1371–1375. DOI: 10.1056/NEJM198705283162204.

[8]   Goldstein JA. Angiographic plaque complexity: the tip of the unstable plaque iceberg. J Am Coll Cardiol. 2002;39:1464–1467. DOI: 10.1016/S0735-1097(02)01772-2

[9]   Tardif JC, Lesage F, Harel F, Romeo P, Pressacco J. Imaging biomarkers in atherosclerosis trials. Circ Cardiovasc Imaging. 2011;4:319–333. DOI: 10.1161/CIRCIMAGING.110.962001

[10] Waxman S, Dixon SR, L'Allier P, Moses JW, Peterson JL, Cutlip D, Tardif JC, Nesto RW, Muller JE, Hendricks MJ, Sum ST, Gardner CM, Goldstein JA, Stone GW, Krucoff MW. *In vivo* validation of a catheter-based near-infrared spectroscopy system for detection of lipid core coronary plaques: initial results of the SPECTACL study. JACC Cardiovasc Imaging. 2009;2:858–868. DOI: 10.1016/l.jcmg.2009.05.001

[11] Cassis LA, Lodder RA. Near-IR imaging of atheromas in living arterial tissue. Anal Chem. 1993;65:1247–1256. DOI: 10.1021/ac00057a023

[12] Wang J, Geng YJ, Guo B, Klima T, Lal BN, et al. Near-infrared spectroscopic characterization of human advanced atherosclerotic plaques. J Am Coll Cardiol. 2002;39:1305–1313. DOI: 10.1016/S0735-1097(02)01767-9

[13] Moreno PR, Muller JE. Identification of high-risk atherosclerotic plaques: a survey of spectroscopic methods. Curr Opin Cardiol. 2002;17:638–647. ISSN: 0268-4705

[14] Jaguszewski M, Klingerberg R. Intracoronary near-infrared spectroscopy (NIRS) imaging for detection of lipid content of coronary plaques: current experience and future perspectives. Curr Cardiovasc Imaging Rep. 2013;6:426–430. DOI:10.1007/s12410-013-9224-2

[15] Erlinge D. Near-infrared spectroscopy for intracoronary detection of lipid-rich plaques to understand atherosclerotic plaque biology in man and guide clinical therapy. J Intern Med. 2015;278:110–125. DOI: 10.1111/joim.12381

[16] Caplan JD, Waxman S, Nesto RW, Muller JE. Near-infrared spectroscopy for the detection of vulnerable coronary artery plaques. J Am Coll Cardiol. 2006;47:C92–96. DOI: 10.1016/j.jacc.2005.12.045

[17] Madder RD, Goldstein JA, Madden SP, Puri R, Wolski K, Hendricks M, Sum ST, Kini A, Sharma S, Rizik D, Brilakis ES, Shunk KA, Petersen J, Weisz G, Virmani R, Nicholls SJ, Maehara A, Mintz GS, Stone GW, Muller JE. Detection by near-infrared spectroscopy of

large lipid core plaques at culprit sites in patients with acute ST-segment elevation myocardial infarction. JACC Cardiovasc Interv. 2013;6:838–846. DOI:10.1016/j.jcin.2013.04.012

[18] Madder RD, Husaini M, Davis AT, Van Oosterhout S, Harnek J, Götberg M, Erlinge D. Detection by near-infrared spectroscopy of large lipid cores at culprit sites in patients with non-ST-segment elevation myocardial infarction and unstable angina. Catheter Cardiovasc Interv. 2015;86:1014–1021. DOI: 10.1002/ccd.25754

[19] de Boer SPM, Brugaletta S, Garcia-Garcia HM, Simsek C, Heo JH, Lenzen MJ, Schultz C, Regar E, Zijlstra F, Boersma E, Serruys PW. Determinants of high cardiovascular risk in relation to plaque-composition of a non-culprit coronary segment visualized by near-infrared spectroscopy in patients undergoing percutaneous coronary intervention. Eur Heart J. 2014;35:282–289. DOI: 10.1093/eurheartj/eht378

[20] Goldstein JA, Maini B, Dixon SR, Brilakis ES, Grines CL, Rizik DG, Powers ER, Steinberg DH, Shunk KA, Weisz G, Moreno PR, Kini A, Sharma SK, Hendricks MJ, Sum ST, Madden SP, Muller JE, Stone GW, Kern MJ. Detection of lipid-core plaques by intracoronary near-infrared spectroscopy identifies high risk of periprocedural myocardial infarction. Circ Cardiovasc Interv. 2011;4:429–437. DOI: 10.1161/CIRCINTERVENTIONS.111.963264

[21] Raghunathan D, Abdel-Karim A-RR, Papayannis AC, daSilva M, Jeroudi OM, Rangan BV, Banerjee S, Brilakis ES. Relation between the presence and extent of coronary lipid core plaques detected by near-infrared spectroscopy with postpercutaneous coronary intervention myocardial infarction. Am J Cardiol. 2011;107:1613–1618. DOI: 10.1016/j.amjcard.2011.01.044

[22] Kini AS, Baber U, Kovacic JC, Limaye A, Ali ZA, Sweeny J, et al. Changes in plaque lipid content after short-term intensive versus standard statin therapy: the YELLOW trial (reduction in yellow plaque by aggressive lipid-lowering therapy). J Am Coll Cardiol. 2013;62:21–29. DOI: 10.1016/j.jacc.2013.03.058

[23] Oemrawsingh RM, Cheng JM, Garcia-Garcia HM, van Geuns R-J, de Boer SPM, Simsek C, et al. Near-infrared spectroscopy predicts cardiovascular outcome in patients with coronary artery disease. J Am Coll Cardiol. 2014;64:2510–2518. DOI: 10.1016/j.jacc.2014.07.998

[24] Jang IK. Near infrared spectroscopy: another toy or indispensable diagnostic tool? Circ Cardiovasc Interv. 2012;5:10–11.DOI: 10.1161/CIRCINTERVENTIONS.111.967935

[25] Jaffer FA, Verjans JW. Molecular imaging of atherosclerosis: clinical state-of-the-art. Heart 2014;100:1469–1477. DOI: 10.1136/heartjnl-2011-301370

[26] Kilic ID, Caiazzo G, Fabris E, Serdoz R, Abou-Sherif S, Madden S, Moreno PR, Goldstein J, Di Mario C. Near-infrared spectroscopy-intravascular ultrasound: scientific basis and clinical applications. Eur Heart J. 2015;16:1299–1306. DOI:10.1093/ehjci/jev208

[27] Dempsey RJ, Davis DG, Buice RG, Lodder RA. Biological and medical applications of near-infrared spectroscopy. Appl Spectrosc OSA. 1996;50:18A–34A. DOI: 10.1366/0003702963906537

[28] Downes A, Elfick A. Raman spectroscopy and related techniques in biomedicine. Sensors. 2010;10:1871–89. DOI: 10.3390/s100301871.

[29] Hanlon EB, Manoharan R, Koo TW, Shafer KE, Motz JT, Fitzmaurice M, Kramer JR, Itzkan I, Dasari RR, Feld MS. Prospects for in vivo Raman spectroscopy. Phys Med Biol. 2000;45:R1–59. DOI: 10.1088/0031-9155/45/2/201

[30] de Lima CJ, Sathaiah S, Silveira L, Zângaro RA, Pacheco MT. Development of catheters with low fiber background signals for Raman spectroscopic diagnosis applications. Artif Organs. 2000;24:231–234. DOI: 10.1046/j.1525-1594.2000.06525.x

[31] Marcu L, Fishbein MC, Maarek JM, Grundfest WS. Discrimination of human coronary artery atherosclerotic lipid-rich lesions by time-resolved laser-induced fluorescence spectroscopy. Arterioscler Thromb Vasc Biol. 2002;21:1244–1250. DOI: 10.1161/hq0701.092091

[32] Toussaint JF, Southern JF, Fuster V, Kantor HL.13C-NMR spectroscopy of human atherosclerotic lesions. Relation between fatty acid saturation, cholesteryl ester content, and luminal obstruction. Arterioscler Thromb. 1994;14:1951–1957. DOI: 10.1161/01.ATV.14.12.1951

[33] Peng S, Guo W, Morrisett JD, Johnstone MT, Hamilton JA. Quantification of cholesteryl esters in human and rabbit atherosclerotic plaques by magic-angle spinning ^{13}C-NMR. Arterioscler Thromb Vasc Biol. 2000;20:2682–2688. DOI: 10.1161/01.ATV.20.12.2682

[34] Trouart TP, Altbach Mi, Hunter GC, Eskelson CD, Gmitro AF. MRI and NMR spectroscopy of the lipids of atherosclerotic plaque in rabbits and humans. Magn Res Med. 1997;38:19–26. DOI: 10.1002/mrm.1910380105

[35] Shydo B, Hendricks M, Frazier G. Imaging of plaque composition and structure with the TVC Imaging System™ and TVC Insight™ catheter. J Invasive Cardiol. 2013;25:5A–8A. ISSN: 1557-2501

[36] Negi SI, Didier R, Ota H, Magalhaes MA, Popma CJ, Kollmer MR, Spad M-A, Torguson R, Suddath W, Satler LF, Pichard A, Waksman R. Role of near-infrared spectroscopy in intravascular coronary imaging. Cardiovasc Revasc Med. 2015;16:299–305. DOI: 10.1016/j.carrev.2015.06.001

[37] Lavine BK, Workman J. Chemometrics. Anal Chem. 2013;85:705–714. DOI: 10.1021/ac303193j

[38] Gardner CM, Tan H, Hull EL, Lisauskas JB, Sum ST, Meese TM, Jiang C, Madden SP, Caplan JD, Burke AP, Virmani R, Goldstein J, Muller JE. Detection of lipid core coronary plaques in autopsy specimens with a novel catheter-based near-infrared spectroscopy system. JACC Cardiovasc Imaging. 2008;1:638–648. DOI: 10.1016/j.jcmg.2008.06.001

[39] Danek BA, Karatasakis A, Madder RD, Muller JE, Madden S, Banerjee S, Brilakis ES. Experience with the multimodality near-infrared spectroscopy/intravascular ultrasound coronary imaging system: principles, clinical experience, and ongoing studies. Curr Cardiovasc Imaging Rep. 2016;9:7. DOI: 10.1007/s12410-015-9369-2

[40] Sum ST, Madden SP, Hendricks MJ, Chartier SJ, Muller JE. Near-infrared spectros-copy for the detection of lipid core coronary plaques. Curr Cardiovasc Imaging Rep. 2009;2:307–415. DOI: 10.1007/s12410-009-0036-3

[41] Lodder RA, Cassis L, Ciurczak EW. Arterial analysis with a novel near-IR fiber-optic probe. Spectroscopy. 1990;5:12–17.

[42] Jarros W, Neumeister V, Lattke P, Schuh D. Determination of cholesterol in athero-sclerotic plaques using near infrared diffuse reflection spectroscopy. Atherosclerosis. 1999;147:327–337. DOI: 10.1016/S0021-9150(99)00203-8

[43] Moreno PR, Lodder RA, Purushothaman KR, Charash WE, O'Connor WN, Muller JE. Detection of lipid pool, thin fibrous cap, and inflammatory cells in human aortic atherosclerotic plaques by near-infrared spectroscopy. Circulation 2002;105:923–927. DOI:10.1161/hc0802.104291

[44] Moreno PR, Ryan SE, Hopkins D, Wise B, Purushothaman KR, Charash WE, O'Connor W, Muller JE. Identification of lipid-rich plaques in human coronary artery autopsy spec-imens by near-infrared spectroscopy. J Am Coll Cardiol. 2001;37:356A. DOI: 10.1016/S0735-1097(01)80005-X

[45] Moreno PR, Ryan SE, Hopkins D. Identification of lipid-rich aortic atherosclerotic plaques in living rabbit with a near infrared spectroscopy catheter. J Am Coll Cardiol. 2001;37:3A. DOI: 10.1016/S0735-1097(01)80001-2

[46] Marshik B, Tan H, Tang J, Lindquist A, Zuluaga A. Discrimination of lipid-rich plaques in human aorta specimens with NIR spectroscopy through whole blood. Am J Cardiol. 2002;90:129H. DOI: 10.1016/S0002-9149(02)02727-3

[47] Marshik B, Tan H, Tang J, Lindquist A, Zuluaga A. Detection of thin-capped fibroath-eromas in human aorta tissue with near infrared spectroscopy through blood. J Am Coll Cardiol. 2003;41:42. DOI :10.1016/S0735-1097(03)80181-X

[48] Waxman S, Tang J, Marshik BJ, Tan H, Khabbaz KR, Connolly RJ, Dunn TA, Zuluaga AF, DeJesus S, Caplan JD, Muller EJ. In vivo detection of a coronary artificial target with a near infrared spectroscopy catheter.Am J Cardiol. 2004;94:141E. DOI: 10.1016/j.amjcard.2004.07.055

[49] Waxman S, Khabba K, Connolly R. Intravascular imaging of atherosclerotic human coro-naries in a porcine model: a feasibility study. Int J Cardiovasc Imaging. 2008;24:37–44. DOI: 10.1007/s10554-007-9227-7

[50] Garcia BA, Wood F, Cipher D, Banerjee S, Brilakis ES. Reproducibility of near-infrared spectroscopy for the detection of lipid core coronary plaques and observed changes after coronary stent implantation. Catheter Cardiovasc Interv. 2010; 76:359–365. DOI: 10.1002/ccd.22500

[51] Abdel-Karim A-RR, Rangan B V, Banerjee S, Brilakis ES. Intercatheter reproducibility of near-infrared spectroscopy for the in vivo detection of coronary lipid core plaques. Catheter Cardiovasc Interv. 2011; 77:657–661. DOI: 10.1002/ccd.22763

[52] Kolodgie FD, Burke AP, Farb A, Gold HK, Yuan J, Narula J, Finn AV, Virmani R. The thin-cap fibroatheroma: a type of vulnerable plaque: the major precursor lesion to acute coronary syndromes. Curr Opin Cardiol. 2001;16:285–292. ISSN: 0268-4705

[53] Rizik D, Goldstein JA. NIRS-IVUS imaging to characterize the composition and structure of coronary plaques. J Invasive Cardiol. 2013;25:2A–4A. ISSN: 1557-2501

[54] Garcia-Garcia HM, Serruys PW. Advances in the invasive diagnosis and treatment of vulnerable coronary plaques. Eur Cardiol Rev 2008;4:105–110. ISSN: 0268-4705

[55] Nissen SE. Halting the progression of atherosclerosis with intensive lipid lowering: results from the Reversal of Atherosclerosis with Aggressive lipid Lowering (REVERSAL) trial. Am J Med. 2005;118:22–27. DOI: 10.1016/j.amjmed.2005.09.020

[56] Nissen SE, Nicholls SJ, Sipahi I, Libby P, Raichlen JS, Ballantyne CM, Davignon J, Erbel R, Fruchart JC, Tardif JC, Schoenhagen P, Crowe T, Cain V, Wolski K, Goormastic M, Tuzcu EM. Effect of very high-intensity statin therapy on regression of coronary atherosclerosis: The asteroid trial. JAMA. 2006;295:1556–65. DOI: 10.1001/jama.295.13.jpc60002

[57] Nicholls SJ, Ballantyne CM, Barter PJ, Chapman J, Erbel RM, Libby P, Raichlen JS, Uno K, Borgman M, Wolski K, Nissen SE. Effect of two intensive statin regimens on progression of coronary disease. N Engl J Med. 2011;365:2078–2087. DOI: 10.1056/NEJMoa1110874

[58] Lee SY, Mintz GS, Kim SY, Hong YJ, Kim SW, Okabe T, Pichard AD, Satler LF, Kent KM, Suddath WO, Waksman R, Weissman NJ. Attenuated plaque detected by intravascular ultrasound clinical, angiographic, and morphologic features and post-percutaneous coronary intervention complications in patients with acute coronary syndromes. JACC Cardiovasc Interv. 2009;2:65–72. DOI: 10.1016/j.jcin.2008.08.022

[59] Guedes A, Tardif JC. Intravascular ultrasound assessment of atherosclerosis. Curr Atheroscler Rep. 2004;6:219–224. DOI: 10.1007/s11883-004-0035-4

[60] Vince DG, Dixon KJ, Cothren RM, Cornhill JF. Comparison of texture analysis methods for the characterization of coronary plaques in intravascular ultrasound imaging. Comput Med Imaging Graph 2000;24:221–229. DOI: 10.1016/S0895-6111(00)00011-2

[61] Kawasaki M, Takatsu M, Noda T, Ito Y, Kunishima A, Arai M, Nishigaki K, Takemura G, Morita N, Minatoguchi S, Fujiwara H. Noninvasive quantitative tissue characterization and two-dimensional color-coded map of human atherosclerotic lesions using ultrasound integrated backscatter: comparison between histology and integrated backscatter images. J Am Coll Cardiol. 2001;38:486–492. DOI: 10.1016/S0735-1097(01)01393-6

[62] Nasu K, Tsuchikane E, Katoh O, Vince G, Virmani R, Surmely JF, Murata A, Takeda Y, Ito T, Ehara M, Matsubara T, Terashima M, Suzuki T. Accuracy of in vivo coronary plaque morphology assessment: a validation study of in vivo virtual histology compared with in vitro histopathology. J Am Coll Cardiol. 2006;47:2405–2412. DOI: 10.1016/j.jacc.2006.02.044

[63] Van Herck G, De Meyer G, Ennekens G, Van Herck P, Herman A, Vrints C. Validation of in vivo plaque characterisation by virtual histology in a rabbit model of atherosclerosis. EuroIntervention 2009;5:149–156.

[64] Stone GW, Maehara A, Lansky AJ, de Bruyne B, Cristea E, Mintz GS, Mehran R, McPherson J, Farhat N, Marso SP, Parise H, Templin B, White R, Zhang Z, Serruys PW. A prospective natural-history study of coronary atherosclerosis. N Engl J Med 2011;364:226–235. DOI: 10.1056/NEJMoa1002358

[65] Calvert PA, Obaid DR, O'Sullivan M, Shapiro LM, McNab D, Densem CG, Schofield PM, Braganza D, Clarke SC, Ray KK, West NE, Bennett MR. Association between IVUS finding and adverse outcomes in patients with coronary artery disease. The VIVA (VH-IVUS in vulnerable atherosclerosis) study. J Am Coll Cardiol Imaging 2011;8:894–901. DOI: 10.1016/j.jcmg.2011.05.005

[66] Kawaguchi R, Oshima S, Jingu M, Tsurugaya H, Toyama T, Hoshizaki H, Taniguchi K. Usefulness of virtual histology intravascular ultrasound to predict distal embolization for ST-segment elevation myocardial infarction. J Am Coll Cardiol. 2007;50:1641–1646. DOI: 10.1016/j.jacc.2007.06.051

[67] Claessen BE, Maehara A, Fahi M, Xu K, Stone GW, Mintz GS. Plaque composition by intravascular ultrasound and distal embolization after percutaneous coronary intervention. JACC Cardiovasc Imaging. 2012;S111–S118. DOI: 10.1016/j.jcmg.2011.11.018

[68] Jang JS, Jin HY, Seo JS, Yang TH, Kim DK, Park YA, Cho KI, Park YH, Kim DS. Meta-analysis of plaque composition by intravascular ultrasound and its relation to distal embolization after percutaneous coronary intervention. Am J Cardiol. 2013;111:968–972. DOI: 10.1016/j.amjcard.2012.12.016

[69] Stone PH, Saito S, Takahashi S, Makita Y, Nakamura S, Kawasaki T, Takahashi A, Katsuki T, Nakamura S, Namiki A, Hirohata A, Matsumura T, Yamazaki S, Yokoi H, Tanaka S, Otsuji S, Yoshimachi F, Honye J, Harwood D, Reitman M, Coskun AU, Papafaklis MI, Feldman CL. Prediction of progression of coronary artery disease and clinical outcomes using vascular profiling of endothelial shear stress and arterial plaque characteristics: the PREDICTION study. Circulation. 2012;126:172–181. DOI: 10.1161/CIRCULATIONAHA.112.096438

[70] Cheng JM, Garcia-Garcia HM, de Boer SP, Kardys I, Heo JM, Akkerhuis KM, Oemrawsingh RM, van Domburg RT, Ligthart J, Witberg KT, Regar E, Serruy PW, van Geuns RJ, Boersma E. In vivo detection of high-risk coronary plaques by radiofrequency intravascular ultrasound and cardiovascular outcome: results of the ATHEROREMO-IVUS study. Eur Heart J. 2014;35:639–647. DOI: 10.1093/eurheartj/eht484

[71] Huang D, Swanson EA, Lin CP, Schuman JS, Stinson WG, Chang W, Hee MR, Flotte T, Gregory K, Puliafito CA, et al. Optical coherence tomography. Science. 1991;254:1178–1181. DOI: 10.1126/science.1957169

[72] Prati F, Regar E, Mintz GS, Arbustini E, Di Mario C, Jang IK, Akasaka T, Costa M, Guagliumi G, Grube E, Ozaki Y, Pinto F, Serruys PW. Expert review document on methodology, terminology, and clinical applications of optical coherence tomography: physical principles, methodology of image acquisition, and clinical application for assessment of coronary arteries and atherosclerosis. Eur Heart J. 2010;31:401–415. DOI: 101093/eurheartj/ehp433

[73] Ozaki Y, Okumura M, Ismail TF, Naruse H, Hattori K, Kan S, Ishikawa M, Kawai T, Takagi Y, Ishii J, Prati F, Serruys PW. The fate of incomplete stent apposition with drug-eluting stents: an optical coherence tomography-based natural history study. Eur Heart J. 2010;31:1470–1476. DOI: 10.1093/eurheartj/ehq066

[74] Onuma Y, Serruys PW, Perkins LE, Okamura T, Gonzalo N, Garcia-Garcia HM, Regar E, Kamberi M, Powers JC, Rapoza R, van Beusekom H, van der Giessen W, Virmani R. Intracoronary optical coherence tomography and histology at 1 month and 2, 3, and 4 years after implantation of everolimus-eluting bioresorbable vascular scaffolds in a porcine coronary artery model: an attempt to decipher the human optical coherence tomography images in the ABSORB trial. Circulation. 2010;122:2288–2300. DOI: 10.1161/CIRCULATIONAHA.109.921528

[75] Radu MD, Falk E. In search of vulnerable features of coronary plaques with optical coherence tomography: is it time to rethink the current methodological concepts? Eur Heart J. 2012;33:9–12. DOI:10.1093/eurheartj/ehr290

[76] Takarada S, Imanishi T, Liu Y, Ikejima H, Tsujioka H, Kuroi A, Ishibashi K, Komukai K, Tanimoto T, Ino Y, Kitabata H, Kubo T, Nakamura N, Hirata K, Tanaka A, Mizukoshi M, Akasaka T. Advantage of next-generation frequency-domain optical coherence tomography compared with conventional time-domain system in the assessment of coronary lesion. Catheter Cardiovasc Interv. 2010;75:202–206. DOI: 10.1002/ccd.22273

[77] Madder RD, Smith JL, Dixon SR, Goldstein JA. Composition of target lesions by near-infrared spectroscopy in patients with acute coronary syndrome versus stable angina. Circ Cardiovasc Interv. 2012;5:55–61. DOI: 10.1161/CIRCINTERVENTIONS.111.963934

[78] Brilakis ES, Banerjee S. How to detect and treat coronary fibroatheroma: the synergy between IVUS and NIRS. JACC Cardiovasc Imaging. 2015;8:195–197. DOI: 10.1016/j.jcmg.2014.11.009

[79] Puri R, Madder RD, Madden SP, Sum ST, Wolski K, Muller JE, Andrews J, King KL, Kiyoko K, Uno K, Kapadia SR, Tuzcu EM, Nissen SE, Virmani R, Maehara A, Mintz GS, Nicholls SJ. Near-infrared spectroscopy enhances intravascular ultrasound assessment of vulnerable coronary plaque. A combined pathological and in vivo study. Arterioscler Thromb Vasc Biol. 2015;35:2423–2431. DOI: 10.1161/ATVBAHA.115.306118

[80] Brugaletta S, Garcia-Garcia HM, Serruys PW, de Boer S, Ligthart J, Gomez-Lara J, Witberg K, Diletti R, Wykrzykowska J, van Geuns RJ, Schultz C, Regar E, Duckers HJ, van Mieghem N, de Jaegere P, Madden SP, Muller JE, van der Steen AF, van der Giessen WJ, Boersma E. NIRS and IVUS for characterization of atherosclerosis in patients undergoing coronary angiography. JACC Cardiovasc Imaging. 2011;4:647–655. DOI: 10.1016/j.jcmg.2011.03.013

[81] Pu J, Mintz GS, Brilakis ES, Banerjee S, Abdel-Karim A-RR, Maini B, Biro S, Lee JB, Stone GW, Weisz G, Maehara A. In vivo characterization of coronary plaques: novel findings from comparing greyscale and virtual histology intravascular ultrasound and near-infrared spectroscopy. Eur Heart J. 2012; 33:372–383. DOI: 10.1093/eurheartj/ehr387

[82] Yonetsu T, Suh W, Abtahian F, Kato K, Vergallo R, Kim SJ, Jia H, McNulty I, Lee H, Jang IK. Comparison of near-infrared spectroscopy and optical coherence tomography for detection of lipid. Catheter Cardiovasc Interv. 2014;84:710–717. DOI: 10.1002/ccd.25084

[83] Roleder T, Kovacic JC, Ali Z, Sharma R, Cristea E, Moreno P, Sharma SK, Narula J, Kini AS. Combined NIRS and IVUS imaging detects vulnerable plaque using a single catheter system: a head-to-head comparison with OCT. EuroIntervention. 2014;10:303–311. DOI: 10.4244/EIJV1013A53

[84] Fur E, Brilakis ES. Comparative intravascular imaging for lipid core plaque: VH-IVUS vs OCT vs NIRS. J Invasive Cardiol. 2013;25:9A–13A. ISSN: 1557-2501

[85] Bourantas CV, Garcia-Garcia HM, Naka KK, Sakellarios A, Athanasiou L, Fotiadis DI, Michalis LK, Serruys PW. Hybrid intravascular imaging, current applications and prospective potential in the study of coronary atherosclerosis. J Am Coll Cardiol. 2013;61:1369–1378. DOI: 10.1016/j.jacc.2012.10.057

[86] Madder RD, Steinberg DH, Anderson D. Multimodality direct coronary imaging with combined near-infrared spectroscopy and intravascular ultrasound: initial US experience. Catheter Cardiovasc Interv. 2013;81:551–557. DOI: 10.1002/ccd.23358

[87] Madder RD, Wohns DH, Muller JE.Detection by intracoronary near-infrared spectroscopy of lipid core plaque at culprit sites in survivors of cardiac arrest. J Invasive Cardiol. 2014;26:78–79. DOI:

[88] Gebhard C, L'Allier PL, Tardif JC. Near-infrared spectroscopy for cardiovascular risk assessment? Not ready for primetime. Eur Heart J. 2014;35:263–265. DOI: 10.1093/eurheartj/eht361

[89] Narula J, Nakano M, Virmani R, Kolodgie FD, Petersen R, Newcomb R, Malik S, Fuster V, Finn AV. Histopathologic characteristics of atherosclerotic coronary disease and implications of the findings for the invasive and noninvasive detection of vulnerable plaques. J Am Coll Cardiol. 2013; 61:1041–1051. DOI: 10.1016/j.jacc.2012.10.054

[90] Patel D, Hamamdzic D, Llano R, Patel D, Cheng L, Fenning RS, Bannan K, Wilensky RL. Subsequent development of fibroatheromas with inflamed fibrous caps can be predicted by intracoronary near infrared spectroscopy. Arterioscler Thromb Vasc Biol. 2013; 33:347–353. DOI: 10.1016/ATVBAHA.112.300710

[91] Kang SJ, Mintz GS, Pu J, Sum ST, Madden SP, Burke AP, Xu K, Goldstein JA, Stone GW, Muller JE, Virmani R, Maehara A. JACC Cardiovasc Imaging. 2015;8:184–194. DOI: 10.1016/j.jcmg.2014.09.021

[92] Oemrawsingh RM, Cheng JM, García-García HM, van Geuns R-J, de Boer SPM, Simsek C, Kardys I, Lenzen MJ, van Domburg RT, Regar E, Serruys PW, Akkerhuis KM, Boersma E. Near-infrared spectroscopy predicts cardiovascular outcome in patients with coronary artery disease. J Am Coll Cardiol. 2014; 64:2510–2518. DOI: 10.1016/j.jacc.2014.07.998

[93] Madder RD, Husaini M, Davis AT, VanOosterhout S, Kan M, Wohns D, McNamara RF, Wolschleger K, Gribar J, Collins JS, Jacoby M, Decker JM, Hendricks M, Sum ST, Madden

S, Ware JH, Muller JE. Large lipid-rich coronary plaques detected by near-infrared spectroscopy at non-stented sites in the target artery identify patients likely to experience future major adverse cardiovascular events. Eur Heart J. 2016;17:393–399.

[94]   Witzenbichler B, Maehara A, Weisz G, Neumann FJ, Rinaldi MJ, Metzger DC, Henry TD, Cox DA, Duffy PL, Brodie BR, Stuckey TD, Mazzaferri EL, Xu K, Parise H, Mehran R, Mintz GS, Stone GW. Relationship between intravascular ultrasound guidance and clinical outcomes after drug-eluting stents: the assessment of dual antiplatelet therapy with drug-eluting stents (ADAPT-DES) study. Circulation. 2014;129:463–470. DOI : 10.1161/ CIRCULATIONAHA.113.003942

[95]   Jang JS, Song YJ, Kang W, Jin HY, Seo JS, Yang TH, Kim DK, Cho KI, Kim BH, Park YH, Je HG, Kim DS. Intravascular ultrasound-guided implantation of drug-eluting stents to improve outcome: a meta-analysis. JACC Cardiovasc Interv. 2014;7:233–243. DOI: 10.1016/j.jcin.2013.09.013

[96]   Ahn JM, Kang SJ, Yoon SH, Park HW, Kang SM, Lee JY, Lee SW, Kim YH, Lee CW, Park SW, Mintz GS, Park SJ. Meta-analysis of outcomes after intravascular ultrasound-guided versus angiography-guided drug-eluting stent implantation in 26,503 patients enrolled in three randomized trials and 14 observational studies. Am J Cardiol. 2012;109:60–66. DOI: 10.1016/j.amjcard.2013.12.043

[97]   Dixon SR, Grines CL, Munir A, Madder RD, Safian RD, Hanzel GS, Pica MC, Goldstein JA. Analysis of target lesion length before coronary artery stenting using angiography and near-infrared spectroscopy versus angiography alone. Am J Cardiol. 2012;109:60–66. DOI: 10.1016/j.amjcard.2011.07.068

[98]   Hanson ID, Goldstein JA, Dixon SR, Stone GW. Comparison of coronary artery lesion length by NIRS-IVUS versus angiography alone. Coron Artery Dis. 2015;26:484–489. DOI: 10.1097/MCA.0000000000000263

[99]   Saeed B, Banerjee S, Brilakis ES. Slow flow after stenting of a coronary lesion with a large lipid core plaque detected by near-infrared spectroscopy. EuroIntervention. 2010;6:545.

[100] Awata M, Kotani J, Uematsu M, Morozumi T, Watanabe T, Onishi T, Iida O, Sera F, Nanto S, Hori M, Nagata S. Serial angiographic evidence of incomplete neointimal coverage after sirolimus-eluting stent implantation: comparison with bare-metal stents. Circulation. 2007;116:910–916. DOI: 10.1161/CIRCULATIONAHA.105.6609057

[101] Waxman S, Freilich MI, Stuer MJ, Shishkov M, Bilazarian S, Virmani R, Bouma BE, Tearney GJ. A case of lipid core plaque progression and rupture at the edge of a coronary stent: elucidating the mechanisms of drug-eluting stent failure. Circ Cardiovasc Interv. 2010;3:193–196. DOI: 10.1161/CIRCINTERVENTIONS.109.917955

[102] Stouffer GA.The use of near-infrared spectroscopy to optimize stent length.J Invasive Cardiol. 2013;25:5A–8A. ISSN: 1557-2501

[103] Joner M, Finn AV, Farb A, Mont EK, Kolodgie FD, Ladich E, Kutys R, Skorija K, Gold HK, Virmani R. Pathology of drug-eluting stents in humans: delayed healing and late thrombotic risk. J Am Coll Cardiol. 2006;48:193–202. DOI: 10.1016/j.jacc.2006.03.042

[104] Oyabu J, Ueda Y, Ogasawara N, Okada K, Hirayama, Kodama K. Angioscopic evaluation of neointima coverage: sirolimus drug-eluting stent versus bare metal stent. Am Heart J. 2006;152:1168–1174. DOI: 10.1016/j.ahj.2006.07.025

[105] Finn AV, Nakazawa G, Ladich E, Kolodgie FD, Virmani R. Does underlying plaque morphology play a role in vessel healing after drug-eluting stent implantation. JACC Cardiovasc Imaging. 2008;1:1485–1488. DOI: 10.1016/j.jcmg.2008.04.007

[106] Nakazawa G, Finn AV, Joner M, Ladich E, Kutys R, Mont EK, Gold HK, Burke AP, Kolodgie FD, Virmani R. Delayed arterial healing and increased late stent thrombosis at culprit sites after drug-eluting stent placement for acute myocardial infarction patients: an autopsy study. Circulation. 2008;118:1138–1145. DOI: 10.1161/CIRCULATIONAHA.107.762047

[107] Otsuka F, Byrne RA, Yahagi K, Mori H, Ladich E, Fowler DR, Kutys R, Xhepa E, Kastrati A, Virmani R, Joner M. Neoatherosclerosis: overview of histopathologic findings and implications for intravascular imaging assessment. Eur Heart J. 2015;36:2147–2159. DOI: 10.1093/eurheartj/ehv205

[108] Ali ZA, Roleder T, Narula J, Mohanty BD, Baber U, Kovacic JC, et al. Increased thin-cap neoatheroma and periprocedural myocardial infarction in drug-eluting stent restenosis: multimodality intravascular imaging of drug-eluting and bare-metal stents. Circ Cardiovasc Interv. 2013; 6:507–517. DOI: 10.1161/CIRCINTERVENTIONS.112.000248

[109] Madder RD, Khan M, Husaini M, Chi M, Dionne S, VanOosterhout S, Borgman A, Collins JS, Jacoby M. Combined near-infrared spectroscopy and intravascular ultrasound imaging of pre-existing coronary artery stents. Can near-infrared spectroscopy reliably detect neoatherosclerosis? Circ Cardiovasc Imaging. 2016;9:e003576. DOI: 10.1161/CIRCIMAGING.115.003576

[110] Ramcharitar S, Gonzalo N, van Geuns RJ, Garcia-Garcia HM, Wykrzykowska JJ, Ligthart JM. First case of stenting of a vulnerable plaque in the SECRIIT I trial-the dawn of a new era? Nat Rev Cardiol. 2009;6:374–378. DOI: 10.1038/nrcardio.2009.34

[111] Finn AV, Joner M, Nakazawa G, Kolodgie F, Newell J, John MC, et al. Pathological correlates of late drug-eluting stent thrombosis: strut coverage as a marker of endothelialization. Circulation. 2007;115:2435–2441. DOI: 10.1161/CIRCULATIONAHA.107.693739

[112] Brugaletta S, Radu MD, Garcia-Garcia HM, Heo JH, Farooq V, Girasis C, et al. Circumferential evaluation of the neointima by optical coherence tomography after ABSORB bioresorbable vascular scaffold implantation: can the scaffold cap the plaque? Atherosclerosis. 2012;221:106–112. DOI: 10.1016/j.atherosclerosis.2011.12.008

[113] Heusch G, Kleinbongard P, Böse D, Levkau B, Haude M, Schulz R, Erbel R. Coronary microembolization: From bedside to bench and back to bedside. Circulation. 2009;120:1822–1836. DOI:10.1161/CIRCULATIONAHA.109.888784

[114] Prasad A, Singh M, Lerman A, Lennon RJ, Holmes DR Jr, Rihal CS. Isolated elevation in troponin T after percutaneous coronary intervention is associated with higher long-term mortality. J Am Coll Cardiol. 2006;48:1765–1770. DOI: 10.1016/j.jacc.2006.04.102

[115] Tanaka A, Kawarabayashi T, Nishibori Y, Sano T, Nishida Y, Fukuda D, Shimada K, Yoshikawa J. No-reflow phenomenon and lesion morphology in patients with acute myocardial infarction. Circulation. 2002;105:2148–2152. DOI: 10.1016/01.CIR.0000015697.59592.07

[116] Limbruno U, De Carolo M, Pistolesi S, Micheli A, Petronio AS, Camacci T, Fontanini G, Balbarini A, Mariani M, De Caterina R. Distal embolization during primary angioplasty: histopathologic features and predictability. Am Heart J. 2005;150:102–108. DOI: 10.1016/j.ahj.2005.01.016

[117] Kotani J, Nanto S, Mintz GS, Kitakaze M, Ohara T, Morozumi T, Nagata S, Hori M. Plaque gruel of atheromatous coronary lesion may contribute to the no-reflow phenomenon in patients with acute coronary syndrome. Circulation. 2002;106:1672–1677. DOI: 10.1161/01.CIR.0000030189.27175.4E

[118] Kawamoto T, Okura H, Koyama Y, Toda I, Taguchi H, Tamita K, Yamamuro A, Yoshimura Y, Neishi Y, Toyota E, Yoshida K. The relationship between coronary plaque characteristics and small embolic particles during coronary stent implantation. J Am Coll Cardiol. 2007;50:1635–1640. DOI: 10.1016/j.jacc.2007.05.050

[119] Goldstein JA, Grines C, Fischell T, Virmani R, Rizik D, Muller J, Dixon SR. Coronary embolization following balloon dilatation of lipid-core plaques. JACC Cardiovasc Imaging. 2009;2:1420–1424. DOI: 10.1016/j.jcmg.2009.10.003

[120] Papayannis AC, Abdel-Karim A-RR, Mahmood A, Rangan B V, Makke LB, Banerjee S, et al. Association of coronary lipid core plaque with intrastent thrombus formation: a near-infrared spectroscopy and optical coherence tomography study. Catheter Cardiovasc Interv. 2013; 81:488–493. DOI: 10.1002/ccd.23389

[121] Schultz CJ, Serruys PW, van der Ent M, Ligthart J, Mastik F, Garg S, et al. First-in-man clinical use of combined near-infrared spectroscopy and intravascular ultrasound: a potential key to predict distal embolization and no-reflow? J Am Coll Cardiol. 2010; 56:314. DOI: 10.1016/j.jacc.2009.10.090

[122] Garcia BA, Wood F, Cipher D, Banerjee S, Brilakis ES. Reproductibility of near-infrared spectroscopy for the detection of lipid core coronary plaques and observed changes after coronary stent implantation. Catheter Cardiovasc Interv. 2010;76:359–365. DOI: 10.1002/ccd.22500

[123] Brilakis ES, Abdel-Karim A-RR, Papayannis AC, Michael TT, Rangan B V, Johnson JL, et al. Embolic protection device utilization during stenting of native coronary artery lesions with large lipid core plaques as detected by near-infrared spectroscopy. Catheter Cardiovasc Interv. 2012; 80:1157–1162. DOI: 10.1002/ccd.23507

[124] Maini A, Buyantseva L, Maini B. In vivo lipid core plaque modification with percutaneous coronary revascularization: a near-infrared spectroscopy study. J Invasive Cardiol. 2013;25:293–295. DOI: PMID: 23735355

[125] Stone GW, Maehara A, Muller JE, Rizik DG, Shunk KA, Ben-Yehuda O, Généreux P, Dressler O, Parvataneni R, Madden S, Shah P, Brilakis ES, Kini AS. Plaque

characterization to inform the prediction and prevention of periprocedural myocardial infarction during percutaneous coronary intervention: the CANARY Trial (Coronary Assessment by Near-infrared of Atherosclerotic Rupture-prone Yellow). JACC Cardiovasc Interv. 2015;8:927–936. DOI: 10.1016/j.jcin.2015.01.032

[126] Vlaar PJ, Svilaas T, van der Horst IC, Diercks GF, Fokkema ML, de Smet BJ, van den Heuvel AF, Anthonio RL, Jessurum GA, Tan ES, Suurmeijer AJ, Zijlstra F. Cardiac death and reinfarction after 1 year in the thrombus aspiration during percutaneous coronary intervention in acute myocardial infarction study (TAPAS): a 1-year follow-up study. Lancet. 2008;371:1915–1920. DOI: 10.1016/S0140-6736(08)60833-8

[127] Frobert O, Lagerqvist B, Olivercrona GK, Omerovic E, Gudnason T, Maeng M, Aasa M, Angeras O, Calais F, Danielewicz M, Erlinge D, Hellsten L, Jensen U, Johansson AC, Karegren A, Nilsson J, Robertson L, Sandhall L, Sjögren I, Ostlund O, Harnek J, James SK. Thrombus aspiration during ST-segment elevation myocardial infarction. N Engl J Med. 2013;369:1587–1597. DOI: 10.1056/NEJMoa1308789

[128] Jolly SS, Cairns JA, Yusuf S, Meeks B, Pogue J, Rokoss MJ, Kedev S, Thabane L, Stankovic G, Moreno R, Gershlick A, Chowdhary C, Lavi S, Niemelä K, Steg PG, Bernat I, Xu Y, Cantor WJ, Overgaard CB, Naber CK, Cheema AN, Welsh RC, Bertrand OF, Avezum A, Bhindi R, Pancholy S, Rao SV, Natarajan K, ten Berg JM, Shestakovska O, Gao P, Widimsky P, Dzavik V. Randomized trial of primary PCI with or without routine manual thrombectomy. N Engl J Med. 2015;372:1389–1398. DOI: 10.1056/NEJMoa1415098

[129] Erlinge D, Harnek J, Goncalves I, Gotberg M, Muller JE, Madder RD. Coronary liposuction during percutaneous coronary intervention: evidence by near-infrared spectroscopy that aspiration reduces culprit lesion lipid content prior to stent placement. Eur Heart J Cardiovasc Imaging. 2015;16:316–324. DOI: 10.1093/ehjci/jeu180

[130] Simsek C, van Geuns RJ, Magro M, Boersma E, Garcia-Garcia HM, Serruys PW. Change in near-infrared spectroscopy of a coronary artery after 1-year treatment with high dose rosuvastatin. Int J Cardiol. 2012;157:e54–e56. DOI: 10.1016/j.ijcard.2011.09.047

[131] Simsek C, Garcia-Garcia HM, van Geuns RJ, Magro M, Girasis C, van Mieghem N, Lenzen M, de Boer S, Regar E, van der Giessen W, Raichlen J, Duckers HJ, Zijlstra F, van der Steen T, Boersma E, Serruys PW. The ability of high dose rosuvastatin to improve plaque composition in non-intervened coronary arteries: rationale and design of the integrated biomarker and imaging study-3 (IBIS-3). EuroIntervention. 2012;8:234–241. DOI: 10.4244/EIJV912A37

[132] Jang IK.Near infrared spectroscopy.Another toy or indispensable diagnostic tool? Circ Cardiovasc Interv. 2012;5:10–11. DOI:10.1161/CIRCINTERVENTIONS.111.967935

[133] Kaul S, Narula J. In search of the vulnerable plaque: is there any light at the end of the catheter? J Am Coll Cardiol. 2014; 64:2519–24.10.1016/j.jacc.2014.10.017

[134] Jang J-S, Song Y-J, Kang W, Jin H-Y, Seo J-S, Yang T-H, et al. Intravascular ultrasound-guided implantation of drug-eluting stents to improve outcome: a meta-analysis. J Am Coll Cardiol Cardiovasc Interv. 2014; 7:233–243. DOI: 10.1016/j.jcin.2013.09.013